Czech Technical University in Prague, Faculty of Mechanical Engineering

Department of Mechanics, Biomechanics and Mechatronics

MASTER’S THESIS

A SIMULATION OF A BODY FALL AS A BASIS FOR A FORENSIC PRACTICE

Prague 2022

Julie Kochanová

ČVUT ČESKÉ VYSOKÉ UČENÍ TECHNICKÉ V PRAZE

ZADÁNÍ DIPLOMOVÉ PRÁCE

I. OSOBNÍ A STUDIJNÍ ÚDAJE

Příjmení: **Kochanová** Jméno: **Julie** Osobní číslo: **466570**

Fakulta/ústav: **Fakulta strojní**

Zadávající katedra/ústav: **Ústav mechaniky, biomechaniky a mechatroniky**

Studijní program: **Aplikované vědy ve strojním inženýrství**

Specializace: **Biomechanika**

II. ÚDAJE K DIPLOMOVÉ PRÁCI

Název diplomové práce:

Simulace pádu těla jako podklad pro forenzní praxi

Název diplomové práce anglicky:

Simulation of body fall as a basis for forensic practice

Pokyny pro vypracování:

Jedná se o pilotní studii problematiky z oblasti forenzní biomechaniky. Student vytvoří zjednodušený 2D model lidského těla. Tento model se bude skládat z těles, které jsou propojeny vazbami a respektují hmotnostní a setrvačné vlastnosti segmentů klidského těla. Cílem simulací bude zjistit výslednou rychlost a zrychlení a sílu dopadu hlavy na zem při různých počátečních podmínkách. Výsledné dopadové parametry budou sloužit ke stanovení indexu - hodnocení poranění mozku a stanovení schopnosti jedince tento náraz po pádu přežít.

Seznam doporučené literatury:

Zatciorsky, V. M. (2002). Kinetics of human motion. Champaign, IL: Humen Kinetics.
Vesely, V., & Vilimek, M. (2012). Head Injury Biomechanics I - Head and Neck Injury. BULLETIN OF APPLIED MECHANICS 8 (32), pp. 65-76.
Straus, J. (2001). Aplikace forenzní biomechaniky. Praha: Police history.
Mariotti, V. G., Golfo, S., Nigrelli, V., & Carollo, F. (2019, October 16). Head Injury Criterion: Mini Review. Am J of Biomed Sci & Res., p. 5 (5).
Franck, H., & Franck, D. (2016). Forensic Biomechanics and Human Injury: Criminal and Civil Applications - An Engineering Approach. CRC Press.

Jméno a pracoviště vedoucí(ho) diplomové práce:

Ing. Miloslav Vilímek, Ph.D., odbor biomechaniky FS

Jméno a pracoviště druhé(ho) vedoucí(ho) nebo konzultanta(ky) diplomové práce:

Datum zadání diplomové práce: **18.11.2021** Termín odevzdání diplomové práce: **16.01.2022**

Platnost zadání diplomové práce: ______________

Ing. Miloslav Vilímek, Ph.D.	doc. Ing. Miroslav Španiel, CSc.	prof. Ing. Michael Valášek, DrSc.
podpis vedoucí(ho) práce	podpis vedoucí(ho) ústavu/katedry	podpis děkana(ky)

III. PŘEVZETÍ ZADÁNÍ

Diplomantka bere na vědomí, že je povinna vypracovat diplomovou práci samostatně, bez cizí pomoci, s výjimkou poskytnutých konzultací.
Seznam použité literatury, jiných pramenů a jmen konzultantů je třeba uvést v diplomové práci.

.

Datum převzetí zadání Podpis studentky

© ČVUT v Praze, Design: ČVUT v Praze, VIC

ANOTACE

Autor:	Julie Kochanová
Název:	Simulace pádu těla jako podklad pro forenzní praxi
Studijní rok:	2021/2022
Studijní program:	Aplikované vědy ve strojním inženýrství
Fakulta:	Fakulta strojní
Ústav:	Ústav mechaniky, biomechaniky a mechatroniky
Specializace:	Biomechanika
Vedoucí:	Ing. Miloslav Vilímek, Ph.D.
Klíčová slova:	forenzní biomechaniky, mechanický model, model lidského těla, pád, numerická simulace, kritérium poranění hlavy
Anotace:	Za pomoci programovacího jazyka Python byl vytvořen zjednodušený 2D mechanický model lidského těla. Do tohoto modelu bylo působeno silou, která představovala sílu úderu. Byly pozorovány hodnoty parametrů při nárazu hlavy na podložku. Zjištěné hodnoty byly vyhodnoceny příslušnými kritérii pro určení závažnosti poranění hlavy.

ANOTATION

Author:	Julie Kochanová
Title:	A Simulation of a fall of a human body
Study year:	2021/2022
Study program:	Applied Sciences in Mechanical Engineering
Faculty:	Faculty of Mechanical Engineering
Institute:	Department of Mechanics, Biomechanics and Mechatronics
Specialization:	Biomechanics
Supervisor:	Ing. Miloslav Vilímek, Ph.D.
Keywords:	forensic biomechanics, mechanical model, human body model, fall, numerical simulation, head injury criterion
Annotation:	A simplified 2D mechanical model of the human body was created using Python programming language. This model was subject to a force that represented the force of a blow. Parameter values were observed when the head struck the pad. The values obtained were evaluated by appropriate criteria for the determined severity of the head injury.

DECLARATION

I hereby declare that I have written this master's thesis independently and quoted all the sources of information used in accordance with methodological instructions on ethical principles for writing an academic thesis. Moreover, I state that this thesis has neither been submitted nor accepted for any other degree.

In Prague, January 2022 ……………………………………

Bc. Julie Kochanová

ACKNOWLEDGEMENTS

I would like to express my sincere gratitude to my supervisor Ing. Miloslav Vilímek, Ph.D. for his patience, motivation, and immense knowledge. His guidance helped me in the time of research and writing of this thesis. I could not have imagined having a better supervisor and mentor for my master's thesis.

CONTENTS

LIST OF SYMBOLS AND ABBREVIATIONS

For a better orientation in marking, scalar quantities are marked in italics, vector quantities in italics and bold, second order tensors only in bold.

Latin symbols

$\boldsymbol{a}$	$[\mathrm{m \cdot s^{-2}}]$	Linear acceleration
$B_{0_S}, B_{1_S}, B_{2_S}$	$[-]$	Coefficients for calculating the weight of a segment
d	$[\mathrm{m}]$	Distance from the axis of rotation
$E_K, E_K{}'$	$[\mathrm{J}]$	Initial and ultimate kinetic energy
f	$[-]$	Coefficient of restitution
$\boldsymbol{F}$	$[\mathrm{N}]$	Force
$\boldsymbol{F_G}$	$[\mathrm{N}]$	Gravitational force
$\boldsymbol{F_n}$	$[\mathrm{N}]$	Axial force
$\boldsymbol{F_t}$	$[\mathrm{N}]$	Friction force
$\boldsymbol{g}$	$[\mathrm{m \cdot s^{-2}}]$	Gravitational acceleration
H	$[-]$	Coefficient for calculating the length of a segment
h_t	$[\mathrm{cm}]$	Total height of the individual
$\mathbf{J}$	$[\mathrm{N \cdot s}]$	Force impulse
I_S	$[\mathrm{kg \cdot m^2}]$	Moment of inertia of the segment
l_s	$[\mathrm{cm}]$	Total length of the individual segment
m	$[\mathrm{kg}]$	Mass
m_s	$[\mathrm{kg}]$	Mass of the segment
m_t	$[\mathrm{kg}]$	Total weight of the individual segment
n_B	$[-]$	Number of bodies in the system
n_C	$[-]$	Number of coupling equations
$\boldsymbol{p}$	$[\mathrm{kg \cdot m \cdot s^{-1}}]$	Momentum
$\boldsymbol{P}, \boldsymbol{P'}$	$[\mathrm{kg \cdot m \cdot s^{-1}}]$	Initial and ultimate momentum
r_s	$[\mathrm{m}]$	Distance from the axis of rotations (segments)
s	$[\mathrm{m}]$	Linear displacement
t	$[\mathrm{s}]$	Time
$\mathbf{T}$	$[\mathrm{N \cdot m}]$	Torque
$\boldsymbol{v}$	$[\mathrm{m \cdot s^{-1}}]$	Linear velocity

Greek symbols

$\boldsymbol{\alpha}$	$[\mathrm{rad}\cdot\mathrm{s}^{-2}]$	Angular acceleration
φ	$[\mathrm{rad}]$	Angle
$\boldsymbol{\omega}$	$[\mathrm{rad}\cdot\mathrm{s}^{-1}]$	Angular velocity

Abbreviations

AIS	Abbreviated Injury Scale
CoM	Center of Mass
DOF	Degrees of Freedom
HIC	Head Injury Criterion
GSI	Gadd Severity Index
TBI	Traumatic Brain Injury

ABSTRACT

A numerical simulation of a fall of a human body was created, which can later be used for forensic practice in the reconstruction of falls. The concept and multibody system and related basic concepts of mechanics are explained at the beginning, without which it would not be possible to create a mechanical model. Then it was stated how to determine the parameters of the human body based on the input information about the person, which was only weight and height. Subsequently, possible injuries due to falls and the criteria used to evaluate the severity of the injury were presented.

A simplified 2D mechanical model of the human body was created using Python programming language. This model consisted of pairs of bodies (segments) that were interconnected by bonds. The input parameters were only the weight and the height of the individual. Based on the knowledge of the input parameters, other necessary parameters were calculated. Subsequently, a force that represented the force of the blow was applied to this model. The behavior of the human body during a fall was observed. The determined values of the parameters were evaluated by the criterion for evaluating the severity of the head injury.

INTRODUCTION

The field of forensic biomechanics is a relatively new field with a rapid development in recent years. This thesis deals with the reconstruction of falls, which are a relatively common application of forensic biomechanics. From a mechanical point of view, a fall is in principle a simple movement that can be analyzed using basic laws of physics. The situation is considerably more complicated if the body reacts with the surrounding structures during falls.

A simple case is a person falling from a window. This raises the question whether the person fell out of the window on their own or whether someone else also influenced their fall. In such cases, it is also necessary to answer questions about third parties, especially in cases with fatal consequences. In the past, there were no such possibilities as today, and therefore it had to be rely only on the knowledge and experience of an expert in dealing with such cases. Nowadays, it is widely used by the reconstruction of falls. These are most often performed by the classic reconstruction method, using test dummies or volunteers.

The problem is that they often do not correspond to the given parameters in terms of their parameters and behavior. Therefore, even the results of these reconstructions are not very reliable. This is the reason why a numerical simulation of the fall of a human body is created and presented in this thesis. This can be used as a basis for forensic practice in the reconstruction of falls.

The aim of this thesis is to introduce the reader to the basic concepts needed to create a 2D mechanical model of a human body. Furthermore, the basic terms describing the solution are explained and defined. Subsequently, a simulation of a falling body is performed by applying different forces (representing blows) to different places on the body and the behavior of the model is observed. The values found when the head hits the mat are evaluated using criteria determining the severity of the head injury.

1 MULTIBODY SYSTEM

The multibody system is a set of rigid bodies that are connected together and can also move independently of each other. Such connection of two rigid bodies is called a kinematic pair and the connection that forms between them is called a joint. (García de Jalón, et al., 1994). In simple terms, this means that if it is moved by the arm in the shoulder, it is also moved by the forearm, the hands, including the fingers. Figure 1 shows the segmented body and shows the hierarchical structure of the multibody system.

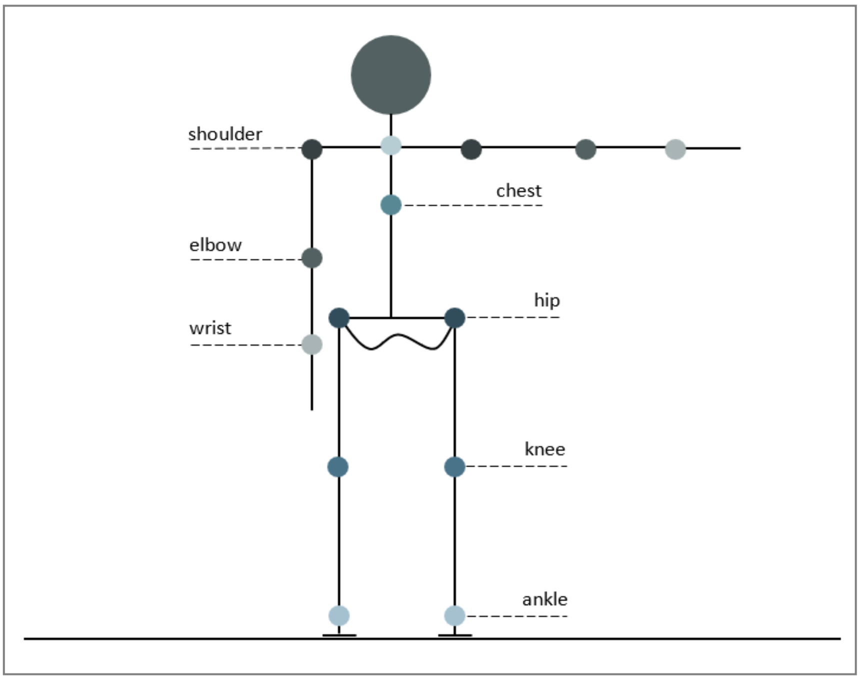

Figure 1 A human body divided into segments

A rigid body means that the considered deformation of the body is regarded to be so small that the deformation has no effect on the movement of the bodies. Therefore, the distance between any two of its rigid body particles remains constant at all times and for all configurations. (Shabana, 2014)

There are several types of joints for joining rigid bodies. The main difference between them is the number of degrees of freedom of relative movement, respectively what movement can be performed in the joint. In the considered 2D space, the body can move without restriction, i.e. it has 3 degrees of freedom and can move in the direction of the X axis, in the direction of the Y axis and rotate.

The multibody system deals with the dynamic behavior of interconnected rigid bodies. Each of these bodies can rotate or move (Figure 2), but it is usually a combination of both movements. A rigid body experiences pure translation, if displacements of any two points on the body are the same. The rigid body rotates around an axis called the axis of rotation and its particles move in parallel levels in circles centered on the same axis.

Therefore, it is clear that in the case of a pure rotation, the points on the rigid body located on the axis of rotation have zero displacement, velocity and acceleration. Pure rotation can be obtained by fixing one point on the body, which is called the base point. (Shabana, 2014)

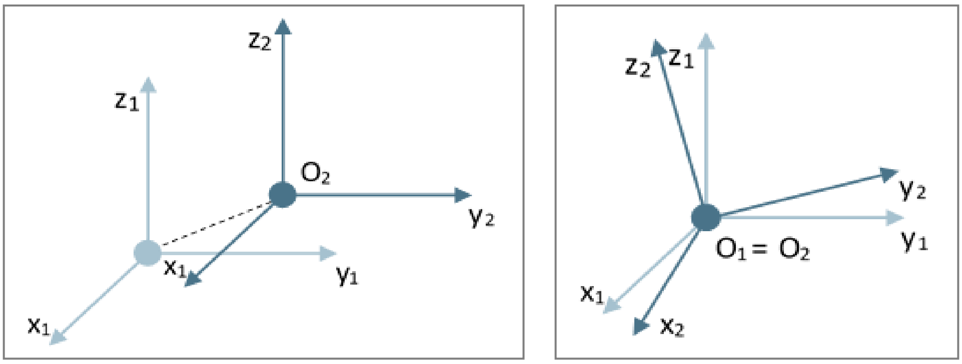

Figure 2 Types of movement: (a) translation, (b) rotation

Mechanical joints reduce the mobility of the multibody system, because the movement of some bodies of the system is dependent on other bodies. This dependence can be mathematically described by a set of nonlinear algebraic constraint equations. And assuming that these constraint equations are linearly independent, then each equation limits the possible motion of the system. The position of each joint is uniquely determined by quantities called degrees of freedom.

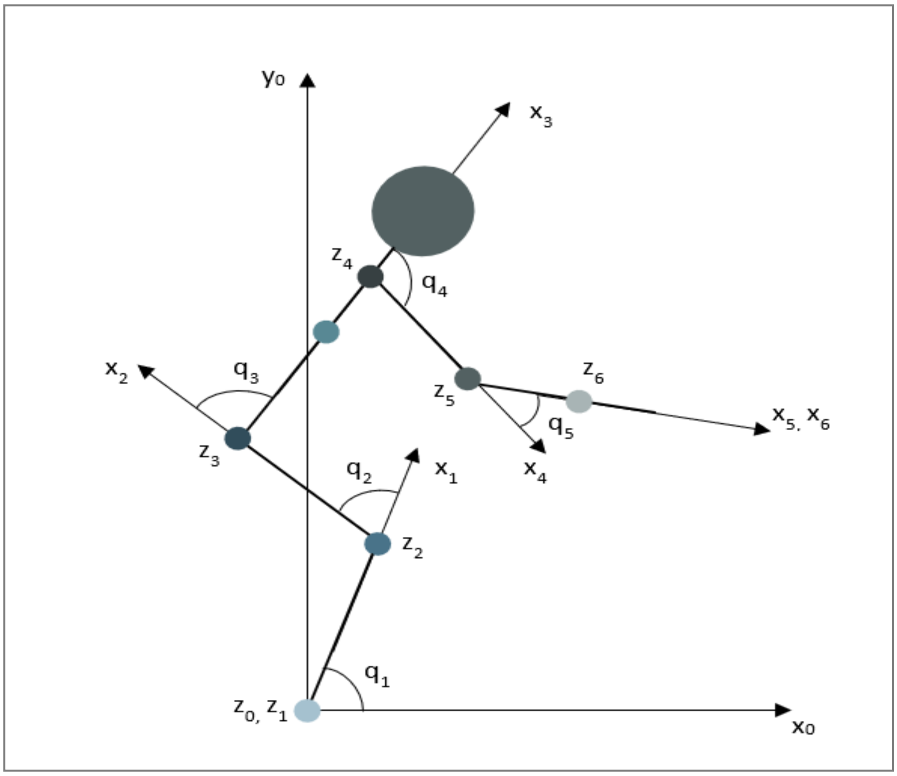

Figure 3 Demonstration of degrees of freedom in the human

Degrees of freedom indicate the number of independent kinematic possibilities of movement. In other words, degrees of freedom represent the minimum number of parameters needed to fully define the position of an entity in space. Therefore, for the system limited n_b solids in two-dimensional space, the number of degrees of freedom can be determined using the Kutzbach criterion as:

$$\mathrm{DOF} = 3 \cdot n_b - n_c, \tag{1}$$

where $n_c$is the number of coupling equations that represent the mechanical connections in the system, as well as the specified motion trajectories. (Shabana, 2014)

The human body is also a multibody system, where the individual anatomical segments represent rigid bodies and the anatomical joints are represented by classical mechanical joints. By adjusting the mobility of the joints in the individual axes, it is possible to prevent the model from getting into an unnatural position.

2 MULTIBODY MECHANICS

The field of physics called mechanics deals with the study of the motion of a multibody system in space and time. According to the relation of the causes of motion, mechanics is divided into kinematics and dynamics. While kinematics studies the motion of objects regardless of the cause of motion, i.e. it deals only with the change of position, velocity and acceleration over time, dynamics deals with the study of objects in motion, which are influenced by moments and forces.

It is important to note that the numerical simulation created later works in discrete steps. And because the step is very small, the following formulas for quantities can be used.

2.1 Kinematics

For simplicity, the segments will be replaced by mass points. The mass point will have the same mass as the body and will be at its center of gravity. Therefore, the movement of the whole body will not be examined, but only the movement of a specific point.

2.1.1 Kinematic Variables

If the mechanical motion of a mass point relative to the selected reference system is described, its position can be determined at any time. The coordinate system in 2D is represented by two orthogonal axes (Figure 4), which are connected at a point called the origin. Using the position vector r, the position of the mass point can be determined. The position vector starts at point O_1 of the coordinate system, which is called the frame of reference, and ends at point O_2 of the object under investigation. The coordinate system moves and rotates with the body, and therefore its position relative to the fixed frame may change.

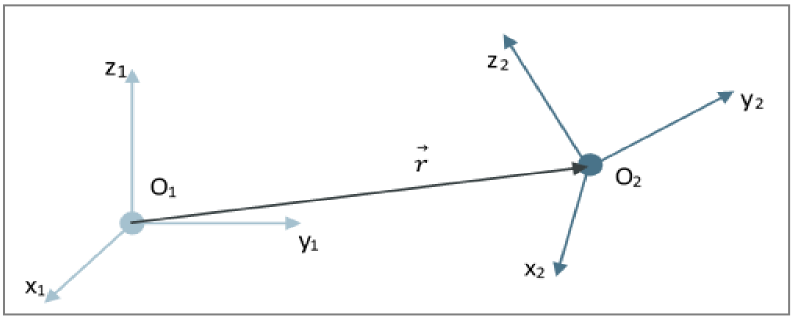

Figure 4 Position of position vector $\vec{r}$ in 2D

Kinematic variables describe the motion of bodies independently of the forces that cause it. The position of a multibody system can be determined using linear and angular displacements, velocities and accelerations. Their values must be measured with respect to the reference frame. (Chow, 2013)

Position

The basic assumption is that in order for a given body or system of bodies to be in motion, it must change its position in the relevant reference frame. The general motion is one that can be decomposed into a sliding and rotating component. In the case of a translational motion, all the mass points of the body have the same velocity and acceleration at the same moment, while in the case of a rotational motion, all the mass points of the body have the same angular velocity. (Nikravesh, 2018)

Velocity

When a change in system position in a reference frame provides information about the state of a rest or moving system, it is the speed of the system, defined as the proportion of the change in position during the time interval Δt:

$$\boldsymbol{v} = \frac{\Delta s}{\Delta t}, \tag{2}$$

where $\boldsymbol{v}$ is the average linear velocity of the body during the analysis time, Δs is the change in linear displacement during the analysis and Δt is the time required to make the linear shift change.

The angular equivalent is:

$$\boldsymbol{\omega} = \frac{\Delta \varphi}{\Delta t}, \tag{3}$$

where $\boldsymbol{\omega}$ is the average angular velocity of the body during the analysis time, $\Delta \varphi$ is the change of angle during the analysis and Δt is the time required to make the linear shift change. (Chow, 2013)

Acceleration

The rate of change of the linear velocity is known as acceleration, with average acceleration being calculated as follows

$$\boldsymbol{a} = \frac{\Delta \boldsymbol{v}}{\Delta t}, \tag{4}$$

where $\boldsymbol{a}$ is the average linear acceleration of the body during the time of analysis, $\Delta \boldsymbol{v}$ is the change in linear velocity over the time of analysis, and Δt is the time taken to undergo the change in linear velocity.

The angular equivalent is:

$$\boldsymbol{\alpha} = \frac{\Delta \boldsymbol{\omega}}{\Delta t}, \tag{5}$$

where $\boldsymbol{\alpha}$ is the average angular acceleration of the body during the time of analysis, $\Delta\boldsymbol{\omega}$ is the change in linear velocity over the time of analysis, and $\Delta t$is the time taken to undergo the change in angular velocity. (Chow, 2013)

2.1.2 Center of Mass

In biomechanical analysis, a human body is often reduced to one known point, the so-called center of gravity (CoM), when describing the movement of the whole body. The center of gravity is the virtual point at which a gravitational force acts on a body, and it is also the point at which a gravitational force acts. (Chow, 2013)

The position of the overall center of gravity of a person is essentially constantly changing, which is caused by a change in the relative position of the individual segments. The human center of gravity can generally be inside or outside the body, depending on the position of the body. However, if the individual is standing in an anatomical position, then the CoM is located exactly in the *planum medianum*, in the small pelvis of the 2nd or 3rd sacral vertebra. Women's CoM is about 1 or 2% lower than men's. (Čihák, 2011)

2.1.3 Equilibrium

An equilibrium position is a position that results from the balance of the forces. In this position, the result of all forces acting on the body is zero (Chow, 2013):

$$\boldsymbol{F} = \boldsymbol{F_1} + \boldsymbol{F_2} + \cdots \boldsymbol{F_n} = \boldsymbol{0} \tag{6}$$

the resultant moment (relative to any axis) is also zero:

$$\boldsymbol{M} = \boldsymbol{M_1} + \boldsymbol{M_2} + \cdots \boldsymbol{M_n} = \boldsymbol{0} \tag{7}$$

2.2 Dynamics

While the chapter on kinematics only dealt with the description of the motion of bodies, without being analyzing what caused the motion, the chapter on dynamics discusses the causes.

2.2.1 Inertia/Moment of Inertia

The term inertia simply means resistance to an action or a change. Similarly, by mechanical definition, inertia is the resistance to acceleration. Inertia is the tendency of a body to maintain its current state of motion, whether it is motionless or moving at a constant speed. Inertia of a human body is directly proportional to its weight. The more mass the object has, the more it tends to maintain its current state of movement, and the more difficult it is to disrupt this state. (Hall, 2011)

Table 1 Lists of moments of inertia (McCaw, 2014)

Description	Figure	Moment of Inertia $[\mathrm{kg \cdot m^2}]$
Solid sphere of radius r_s and mass of the segment m_s.	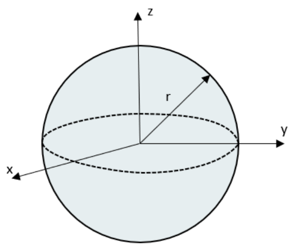	$I_s = \frac{2}{5} \cdot m_s \cdot {r_s}^2$
Thin segment of length l_s and mass m_s, perpendicular to the axis of rotation, rotating about one end.	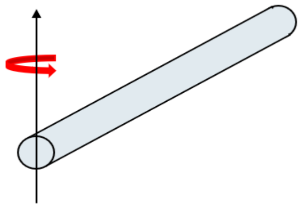	$I_s = \frac{1}{3} \cdot m_s \cdot {l_s}^2$

2.2.2 Force

Force does not cause movement but causes a change in the state of a movement. If a force is applied to the body, it is set in motion or its movement accelerates. It is also possible to slow down the movement or bring the body to a rest. The force can be represented as pressure or tension acting on the body. Each force is characterized by its magnitude, direction and place in which it acts. The law of acceleration, which describes motion for any moment and at any time, is defined as:

$$\boldsymbol{F} = m \cdot \boldsymbol{a} = m \cdot \frac{d\boldsymbol{v}}{dt}, \tag{8}$$

where $\boldsymbol{F}$ is a force, m is the mass of the body and $\boldsymbol{a}$ is the acceleration of the body. It appears that mass is also closely connected with the term force. The mass m, in the metric system with the unit kg, characterizes the inertial properties of bodies. (Chow, 2013)

Gravitational force

It is the force that the Earth exerts on each body, and its magnitude is affected by latitude. If the body is not on the ground but is falling - it moves in free-fall. Free-fall is a uniformly accelerated motion with constant acceleration g called gravitational acceleration. The gravitational force $\boldsymbol{F_G}$ is defined using Newton´s second law (8), where m is the mass of the body and instead of acceleration, gravitational acceleration $\boldsymbol{g}$ is substituted, then:

$$\boldsymbol{F_G} = m \cdot \boldsymbol{g} \tag{9}$$

Gravitational force always has a direction vertically downwards, perpendicular to the Earth's surface.

Frictional force

Frictional force is one of the forces that acts against the direction of the movement of the body and creates resistance (prevents its movement). If one body moves on the surface of another body and there is a shear friction f. The resistance force that breaks such movement is called friction force $\boldsymbol{F_t}$ and acts on the surface of moving bodies. Friction force is directly proportional to the axial force $\boldsymbol{F_n}$, which the body acts perpendicular to the pad. The proportionality constant is the coefficient of shear friction *f*:

$$\boldsymbol{F_t} = f \cdot \boldsymbol{F_n}, \tag{10}$$

The coefficient of shear friction is a dimensionless number, which describes a relationship between a pair of materials that move on top of each other. (Chow, 2013)

Torque

Closely related to the term force is the rotational effect created by an eccentric force known as the torque $\boldsymbol{T}$ or torque. The torque expresses the action of the force $\boldsymbol{F}$ on a point remote from the axis of rotation d, the relationship then looks as follows:

$$\boldsymbol{T} = \boldsymbol{F} \cdot d \tag{11}$$

The greater the torque acting on the axis of rotation, the greater the tendency to rotate.

2.2.3 Momentum of a body

Momentum of a body *p* is given by the product of its mass m and its velocity *v.* It is a vector that has the same direction as the instantaneous velocity:

$$\boldsymbol{p} = m \cdot \boldsymbol{v} \tag{12}$$

If the momentum change occurs due to a change in velocity direction, then the momentum change relationship must be written in vector form:

$$\Delta \boldsymbol{p} = \int_{v_0}^{v} m \, d\boldsymbol{v} \tag{13}$$

The concept of body momentum is very closely related to the law of conservation of momentum. This says that if two bodies are put out of motion by mutual force action, then the sum of their momentum remains constant (is zero), i.e., the same as before the motion. (Chow, 2013)

2.2.4 Impulse of force

The greater the force applied, the greater the change in momentum. It is also important how long this force lasts. It is apparent that, the longer the force acts, the greater the change in momentum:

$$\boldsymbol{F}\Delta t = \Delta \boldsymbol{p} = m\Delta \boldsymbol{v} \tag{14}$$

This formulation of the force impulse is valid only if the applied force is constant in the time interval Δt. However, if the force is variable, then it is necessary to move from a final interval of time Δt to an infinitesimal interval dt. In such a short time, the force is considered constant, and the following applies to the force impulse:

$$\boldsymbol{F}\, dt = \mathrm{d}\boldsymbol{p} \tag{15}$$

If a force impulse is to be determined and thus a change in momentum in a final time interval, for example from time t_0 to time t, then the last equation must be integrated:

$$\int_{t_0}^{t} \boldsymbol{F}\, dt = \int_{p_0}^{p} \mathrm{d}\boldsymbol{p} \tag{16}$$

In equation (16), the left side represents the force impulse $\boldsymbol{J}$ and the right side is calculated for the case of constant weight m:

$$\boldsymbol{J} = \int_{t_0}^{t} \boldsymbol{F}\, dt = m\boldsymbol{v} - m\boldsymbol{v_0} \tag{17}$$

The time effect of a force (force impulse) acting on an object causes a change in its momentum. (Chow, 2013)

2.2.5 Equations of motion

The equation of motion describes a mathematically dynamic process that determines the possible motions of a body in a given environment. A body is understood to mean, for example, a conventional rigid body or a system of bodies. While the environment is mainly represented by forces and force fields acting on the body and mechanical bonds that limit its movement. Each body can be replaced by a single mass point, in the case of a multibody system by a system of mass points. (Stejskal, et al., 2001)

The motion of a mass point or a system of mass points can be investigated using the release method. According to the principle of this method, each material point in the system behaves the same as a lone point after its release from the system and after the connection of the force effects of the bonds (reactions). Figure 5 shows the release of the multibody system to individual bodies. The resulting Free Body diagram must show all forces, moments and reactions acting on the segment. (Hall, 2011)

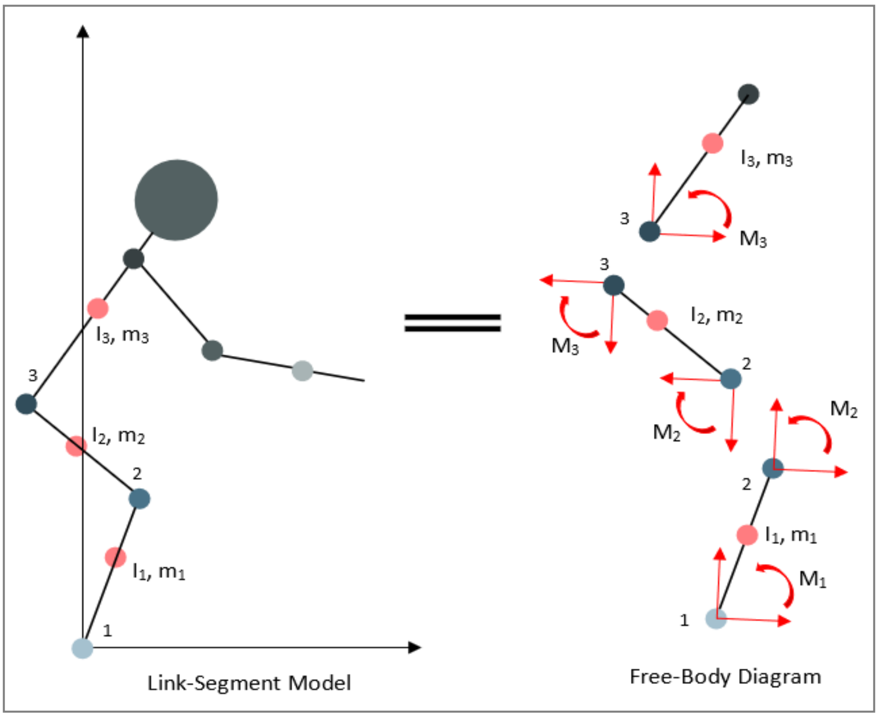

Figure 5 Method of releasing a system of bodies

It is possible to compile a basic equation of motion for each body. These determine the relationship between the forces acting on a material object and the motion caused by those forces. By excluding reactions, the own equations of motion are obtained. A system of second-order differential equations called Newton-Euler equations is used to describe the motion of individual bodies (Chow, 2013):

$$\sum \boldsymbol{F} = m\boldsymbol{a}, \tag{18}$$

$$\sum \boldsymbol{M} = \boldsymbol{I_s}\ddot{\boldsymbol{\varphi}} + \boldsymbol{\omega} \times \boldsymbol{I_s}\boldsymbol{\omega}, \tag{19}$$

3 COLLISION

A collision is defined as a short-term interaction between two or more bodies at the same time. As a result of the collision, internal forces are created which can cause the body to deform at the point of contact. Among other things, it also changes the movement and the velocity of the bodies involved.

A simple example is the oblique impact of two spheres shown in Figure 6. The oblique impact means that the vectors of both bodies do not lie on the same line but intersect each other. The spheres considered will have a mass m_A, m_B and initial velocity $\boldsymbol{v}_{\boldsymbol{A}_y}$, $\boldsymbol{v}_{\boldsymbol{B}_y}$.The moment at which both spheres touch is called the contact point. At this point, a contact force acts between the bodies, which compresses the two spheres with each other and thus reduces the distance between the centers of mass. This is the first stage that ends when the distance between the centers of gravity is the smallest and the contact force is the greatest. This is followed by the restitution stage. (Menčík, 2018)

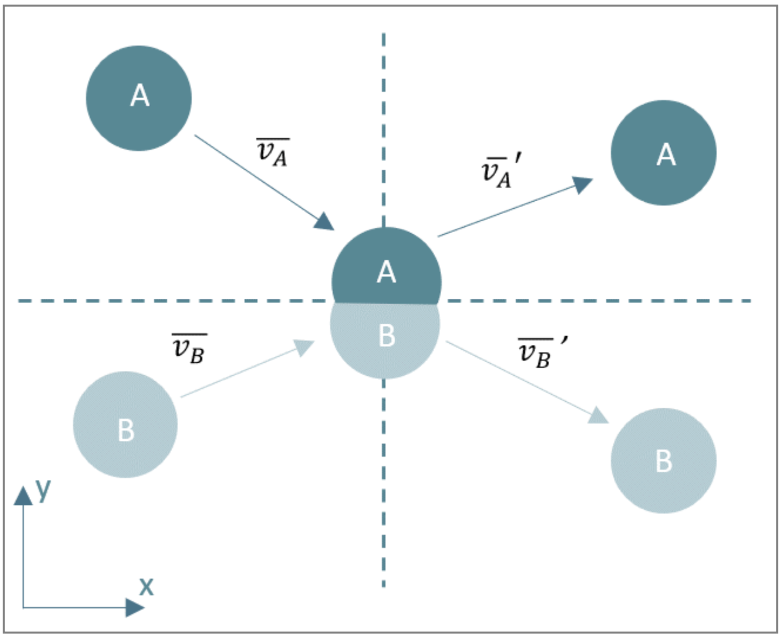

Figure 6 Collision in 2D – Impact of two bodies

There are different types of collisions that differ in whether the kinetic energy is conserved or not. If the kinetic energy of the collision is preserved, then these collisions are called elastic. In contrast, inelastic collisions do not store any kinetic energy. That is, if $\boldsymbol{P}$ and $E_K$represent the initial momentum and kinetic energy before the collision and $\boldsymbol{P}'$and E_K' are the ultimate momentum and kinetic energy after the collision, then (Chow, 2013):

elastic collisions: $$\boldsymbol{P} = \boldsymbol{P}' \text{ and } E_K = E_K' \quad (20)$$

inelastic collisions: $$\boldsymbol{P} = \boldsymbol{P}' \text{ and } E_K \neq E_K' \quad (21)$$

If the deformations are only elastic, then in the first stage, part of the kinetic energy changes into the potential energy of elastic stresses. In the next stage, this energy is released, and the deformations decrease, after a while the bodies separate and continue at different velocities $\boldsymbol{v'}_{\boldsymbol{A}_y}$, $\boldsymbol{v'}_{\boldsymbol{B}_y}$.In this case, it is an elastic collision. While if no release occurs, it is inelastic. These are two extreme situations that do not normally occur. In the real world, a semi-elastic impact occurs, during which only partial suspension occurs. (Menčík, 2018)

3.1 Coefficient of Restitution

The measure of the extent to which kinetic energy is preserved during reflection is the restitution coefficient. Although it is not a property of the material, its value can be predicted on the basis of material properties and impact velocity. (Menčík, 2018)

The definition of the coefficient of restitution is relatively simple, it is the ratio of the final velocity to the initial velocity between two objects after their collision. When deriving the formula for calculating the coefficient of restitution f, two objects will be considered, object A and object B. For both cases, the initial velocity and the velocity after the collision are known. (Chow, 2013)

Although there are several types of collisions, the law of conservation of momentum applies to all of them, i.e.:

$$\boldsymbol{P_A} + \boldsymbol{P_B} = \boldsymbol{P'_A} + \boldsymbol{P'_B} \tag{22}$$

and therefore, it can be described as follows:

$$m_A \boldsymbol{v}_{\boldsymbol{A}_y} + m_B \boldsymbol{v}_{\boldsymbol{B}_y} = m_A \boldsymbol{v'}_{\boldsymbol{A}_y} + m_B \boldsymbol{v'}_{\boldsymbol{B}_y} \tag{23}$$

where m_A, m_B is mass of objects, $\boldsymbol{v}_{\boldsymbol{A}_y}$, $\boldsymbol{v}_{\boldsymbol{B}_y}$are the initial velocities of objects and $\boldsymbol{v'}_{\boldsymbol{A}_y}$, $\boldsymbol{v'}_{\boldsymbol{B}_y}$are the velocities of the objects after the collision. And because the restitution coefficient is defined as the ratio of the final and initial relative velocities between two objects (in this case, object A and object B), it can be expressed mathematically as:

$$f = \frac{|\boldsymbol{v'_b} - \boldsymbol{v'_a}|}{|\boldsymbol{v_a} - \boldsymbol{v_b}|}, \tag{24}$$

where f is the coefficient of restitution. (Chow, 2013)

The extent to which the collision is elastic or inelastic is determined by the coefficient of restitution f. The value of the coefficient of restitution is between zero and one. While a perfectly elastic collision has a coefficient of restitution of one, in the case of a perfectly inelastic collision its value is zero. In the real world, its value is always between these two limits. (Chow, 2013)

4 MATHEMATICAL SOLUTION

Physics engines are used to simulate the physical world. The physical engines description main use is in the field of computer games and scientific simulations, as they are able to mimic the behavior of solid objects (*rigid body dynamics*), their destruction and collision detection. When choosing a suitable physical engine, it is necessary to choose a compromise between accuracy and speed, depending on the requirements of the target application. If simulations of kinematics, dynamics and collisions of rigid bodies are sufficient, almost any system can be used.

The basis of simple game simulations is a particle system. In general, each particle has two main variables, i.e., its position and velocity. From the mathematical point of view, the change of quantities can be described using differentials and derivatives. By expressing the relations between functions, their differentials and derivatives, differential equations describing the change of phenomena are obtained. There are several numerical methods that are used to solve ordinary differential equations. The most well-known methods include Euler's and Verlet's methods. While Euler's method stores the position and velocity of each particle at each step, Verlet's method stores the current and previous position. Each of them has its advantages and disadvantages, however, Verlet's method of integration is used in game simulations more often. (Gilat, et al., 2013)

4.1 Numerical Solution of Ordinary Differential Equations

First-order differential equations in which the derivative is directly expressed will be considered. It will be looking for a real function $y(x)$ which would be valid in the following equation:

$$\frac{dy(x)}{dx} = f(x, y) \tag{25}$$

This equation is called the initial (Cauchy) problem and can be written in the form:

$$y' = f(x, y) \tag{26}$$

There are many functions which meet the criteria of this equation. One specific solution can be determined using the initial condition, which is a necessary part of the task assignment. It is given in the form:

$$y(x_n) = y_n, \tag{27}$$

where x_n, y_n are the given values. As the algorithm works with discrete data, the solution sought is calculated in discrete time points x_0, x_1, x_2, …, x_n. The intervals between these points are called integration steps:

$$h = x_{n+1} - x_n \tag{28}$$

The numerical solution of the differential equation is based on the point x_n, its value is given by the initial condition. The solution is sought in points x_{n+1} and then an estimate of the exact solution y_n is obtained at these points.

If only one previous value is used for the calculation, then this method is called one-step. However, if n previous points are used for the calculation, it is a multi-step method (*n-step*). The problem of multi-step methods is their so-called initialization values, which are not known for the first few steps in the calculation. One of the one-step methods is usually used to calculate the first N steps.

There are several types of numerical methods to choose from when solving ordinary differential equations. Numerical methods can be compared with each other based on several criteria/their characteristics. One of them is the accuracy of the method, i.e., the size of the local error. In general, higher-order methods are more accurate (have a smaller local error) than lower-order methods of the same type. Another important characteristic is the stability of the method and its usability. In addition, the time-consuming nature of the calculation plays a key role in the decision-making process, when the speed of the solution is inversely proportional to the order of the method for a given integration step h. Multi-step methods in a given integration step are faster than one-step methods. And an equally important criterion is memory requirements. The demands that the method puts on memory are directly proportional to the order of the method.

4.2 Explicit Euler's Method

Euler method is one of the basic methods used for numerical solution of ordinary differential equations with initial conditions. It can be included in the group of one-step discrete methods. The method uses only the value from the previous step, which can be called the default step, to calculate the new value (Gilat, et al., 2013)

The explicit Euler method is derived using Taylor expansion, i.e., the formula is used:

$$y(x_{n+1}) = y(x_n) + \frac{h}{1!}\frac{dy(x_n)}{dt} + \mathcal{O}(h^2) \tag{29}$$

and therefore

$$y'(x_n) = \frac{dy(x_n)}{dt} = \frac{y(x_{n+1}) - y(x_n)}{h} + \mathcal{O}(h) \tag{30}$$

If the relation $y'(x_n) = f(x_n, y(x_n))$ is used, if the expression $\mathcal{O}(h)$ is neglected and if the values $y(x_i)$ of the exact solution are replaced by the values y_i of the approximate solution, then it is obtained the following equation (30) relationship:

$$\frac{y_{n+1} - y_n}{h} = f(x_n, y_n) \tag{31}$$

By expressing y_{n+1}a relation is obtained for the explicit Euler method:

$$y(x_{n+1}) = y_n + hf(x_n, y_n) \tag{32}$$

In Figure7 Explicit Euler´s method, Euler's method is shown as a graph. For clarity, the solution of the differential equation is plotted in blue in the graph, although it is not actually known. The coordinate point $(x_n, y_n)$is given by the initial condition (27). The value of the independent variable for the next solution point is determined by Equation (28). The coordinate values are set to the starting point to the right side of equation (26) and the result is the direction of the tangent at the starting point $y_n' = f(x_n, y_n)$.Using Euler's formula (32), the intersection of the tangent with the perpendicular at the point x_n is found. The calculated point is considered the starting point and the method for calculating other points is similar. It is clear from the figure that the numerical solution from a graphical point of view replaces the continuous curve of the analytical solution with a polyline. (Gilat, et al., 2013)

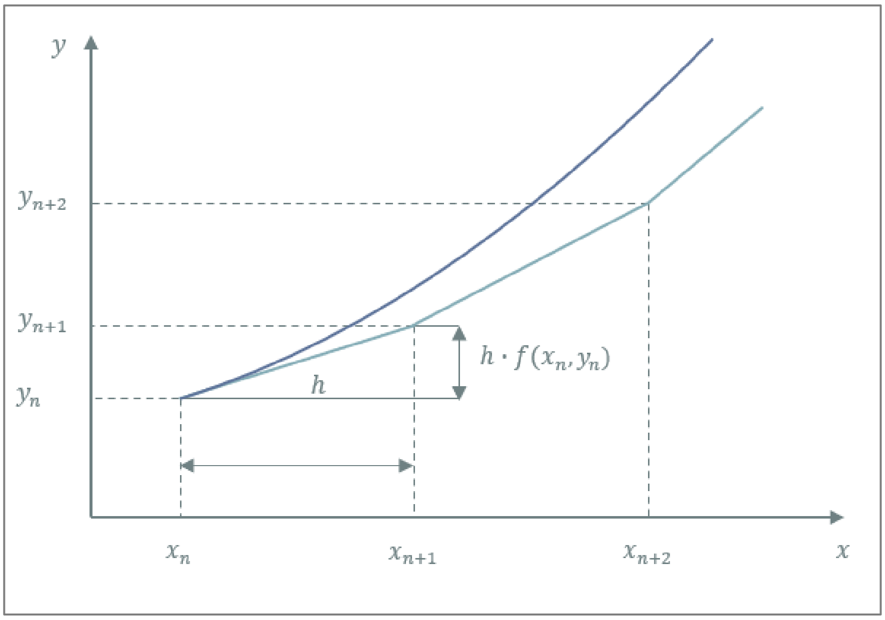

Figure7 Explicit Euler´s method

Although Euler's method is considered a simple numerical method, it is rarely used. The big disadvantage is its error rate, which increases with each step. Errors are accumulated in individual steps so that there is a complete loss of accuracy. This makes the method highly unstable. To determine the magnitude of the error, the Taylor polynomial will again be used, in which the function $\mathcal{O}$ gives the value of the difference between the actual value and the approximation. The Taylor development used looks like this:

$$y(x_{n+1}) = y(x_n) + \frac{h}{1!}\frac{dy(x_n)}{dt} + \frac{h^2}{2!}\frac{d^2y(x_n)}{dt^2} + \mathcal{O}(h^3) \tag{33}$$

The error of Euler's method is given by the difference between equations (29) and (32). Obviously, the difference from the actual value depends on the square of the step size h. This means that halving the step size means reducing the error by only a quarter. The total error then depends on the size of step h and the number of steps N. (Gilat, et al., 2013)

The advantage of Euler's method lies in its simplicity and the speed of solution; however, its residual error reaches large values and is therefore not suitable for accurate calculations of differential equations.

4.3 Implicit Euler's Method

By simply modifying the explicit Euler method, the earlier mentioned stability problems can be eliminated. The difference is that the implicit Euler method evaluates the function f in the end step instead of the starting point. The form of the backward Euler method is:

$$y(x_{n+1}) = y_n + hf(x_{n+1}, y_{n+1}) \tag{34}$$

Compared to the explicit method, the implicit method is more stable but slower. Therefore, even this method is not suitable for scientific simulations. (Gilat, et al., 2013)

4.4 Semi-implicit Euler Method

Another modification of the Euler method that helps with stability is the semi-implicit Euler method. It is also sometimes called symplectic Euler. It is a sympathetic integrator and therefore gives better results than the explicit Euler method. The new velocity is calculated first:

$$\frac{\mathrm{y}(x_{n+1}) - \dot{y}(x_n)}{h} = f(x_n, y_n, \dot{y}(x_n)) \tag{35}$$

and then a new position is calculated using its calculated value:

$$\frac{y(x_{n+1}) - y_n}{h} = \mathrm{y}(x_{n+1}) \tag{36}$$

Although this method is more stable than the explicit Euler method, it is not as stable as the implicit Euler method. (Catto, 2015)

4.5 Verlet's Method

The derivation of the Verlet algorithm is similar to Euler's method on Taylor's expansion $y(t)$. It is assumed that the function $f(t, y)$ is analytic around the point (t_0, y_0). Then in this area there is an analytical solution of the differential equation (25) in the form:

$$y(x) = y(x_n) + \frac{h}{1!}\frac{dy(x_n)}{dt} + \frac{h^2}{2!}\frac{dy^2(x_n)}{dt^2} + \frac{h^3}{3!}\frac{dy^3(x_n)}{dt^3} + O(h^4) \tag{37}$$

and then for sufficiently small h the following equations will apply:

$$\mathrm{y}(x_{n+1}) = \mathrm{y}(x_n) + \dot{y}(x_n)h + \frac{1}{2}\ddot{y}(x_n)h^2 + \frac{1}{6}y^{(3)}h^3 + \mathcal{O}(h^4) \tag{38}$$

$$y(x_{n-1}) = y(x_n) - \dot{y}(x_n)h + \frac{1}{2}\ddot{y}(x_n)h^2 - \frac{1}{6}y^{(3)}h^3 + \mathcal{O}(h^4) \tag{39}$$

Equation (38) expresses a step forward in time, while Equation (39) a step back in time. By summing these two equations and leaving the relationy(x_{n+1}) on the left side, the equation is obtained:

$$\mathrm{y}(x_{n+1}) + \mathrm{y}(x_{n-1}) = 2\mathrm{y}(x_n) + \ddot{y}(x_n)h^2 + \mathcal{O}(h^4), \tag{40}$$

therefore (Catto, 2015):

$$\mathrm{y}(x_{n+1}) \approx 2\mathrm{y}(x_n) - y(x_{n-1}) + \ddot{y}(x_n)h^2 \tag{41}$$

To calculate the new position, it is sufficient to know the previous and current positions of the point (particle) and the acceleration that acts on it. Verlet's method is therefore a two-step method. The problem of the initialization method for the previous position can be solved by using the Euler method for the first step and thus starting the method appropriately.

Thanks to the use of the Verlet method, the speed of the calculation is completely omitted, which considerably reduces the error rate of this method. Although the method is not always accurate, it is suitable for real-time particle simulation. In addition, it is easy to use in simple game simulations. (Van Verth James, 2015)

5 ANTHROPOMETRY

Anthropometry is a major field in anthropology that studies physical measurements of the human body and determines the differences between individuals and groups. A wide range of physical measures is needed to describe and distinguish characteristics of race, gender, age, or a body type. However, parameters such as mass, moment of inertia and its location are sufficient to describe human movement. (Winter, 2009) The knowledge of the field of anthropometry will be used to calculate the parameters of individual segments of a human body.

5.1 Weight of Individual Segments

The mass of individual segments of a human body can be determined using the method of Zatciorsky and Selujanov (1979). The method is based on their research, who experimentally determined the coefficients on the basis of research of 100 persons by radio isotropic method. Since all these values were determined experimentally, their generalization is made with a certain probability and burdened by a certain measurement error. The weight of individual body segments can be determined by knowing the total weight [kg] and total height [cm] of individuals. The mass of a given segment can be calculated using an equation:

$$m_s = B_{0_s} + B_{1_s} \cdot m_t + B_{2_s} \cdot h_t, \tag{42}$$

where $m_t[\mathrm{kg}]$ is the total weight of the individual, $h_t[\mathrm{cm}]$ is the total height of the individual and B_{0_s}, B_{1_s} aB_{2_s} are coefficients which they were determined experimentally (Table 2).

Table 2 The weight of individual segments (Zatciorsky, et al., 1983)

Segment	$\mathrm{B_0}$ [kg]	$\mathrm{B_1}$	$\mathrm{B_2}$ [$\mathrm{kg \cdot cm^{-2}}$]
Head	1.2960	0.0171	0.0143
Trunk - upper part	8.2144	0.1826	-0.0584
Trunk – middle part	7.1810	0.2234	-0.0663
Trunk – lower part	-7.4980	0.0976	0.04896
Thigh	-2.6490	0.1463	0.0137
Calf	-1.5920	0.03616	0.0121
Foot	-0.8290	0.0077	0.0073
Upper arm	0.2500	0.03013	-0.0027
Forearm	0.3184	0.01445	-0.00114
Hand	-0.1165	0.0036	0.00175

To check that the total weight of an individual is equal to the sum of the weights of the individual segments, it is enough to add these weights - just be aware that some limbs must be counted twice. Table 3 is designed to control the weight fraction of individual segments.

Table 3 The weight share of individual segments (Zatciorsky, 2002)

Segment	Optimum	Min	Max
Head	0.074	0.0568	0.0886
Trunk - upper part Trunk – middle part Trunk – lower part	0.448	0.4028	0.5070
Thigh	0.124	0.0970	0.1473
Calf	0.046	0.0399	0.0530
Foot	0.016	0.0114	0.0210
Upper arm	0.029	0.0259	0.0336
Forearm	0.017	0.0153	0.0228
Hand	0.007	0.0054	0.0100

5.2 Length of Segments

Using the parameter of the length of individual segments between the joints, it is possible to determine where the center of gravity of individual segments is located. The following formula was used to calculate the length of the segments (Winter, 2009):

$$l_s = h_t \cdot H, \tag{43}$$

where $l_s[\mathrm{cm}]$ is the total length of the individual segment, $h_t[\mathrm{cm}]$ is the total height of the individual and H are the coefficients (Table 4).

Table 4 The length of segments

Segment	Value of parameter H		Segment	Value of parameter H
Head	0.182		Calf	0.246
Trunk - upper part Trunk – middle part Trunk – lower part	0.288		Foot Upper arm Forearm	0.039 0.186 0.146
Thigh	0.245		Hand	0.108

5.3 Center of Gravity of Individual Segments

The position of the center of gravity of a–body shows the distribution of its weight. Its definition is based on the zero sum of static moments of partial masses to the position of the center of gravity of the body. The total center of gravity changes with the change of the position of individual bodies. The overall center of gravity of the body is related to the stability of a person in individual postures and positions.

The position of the center of mass can be determined based on knowledge of the individual's height and on the percentage distribution of the position as shown in Figure 8 (Winter, 2009)

The position of the total center of mass varies depending on the weight ratio of the individual, and even the total center of gravity does not have to be inside the body. The overall center of mass is related to the stability of a person in individual postures and positions.

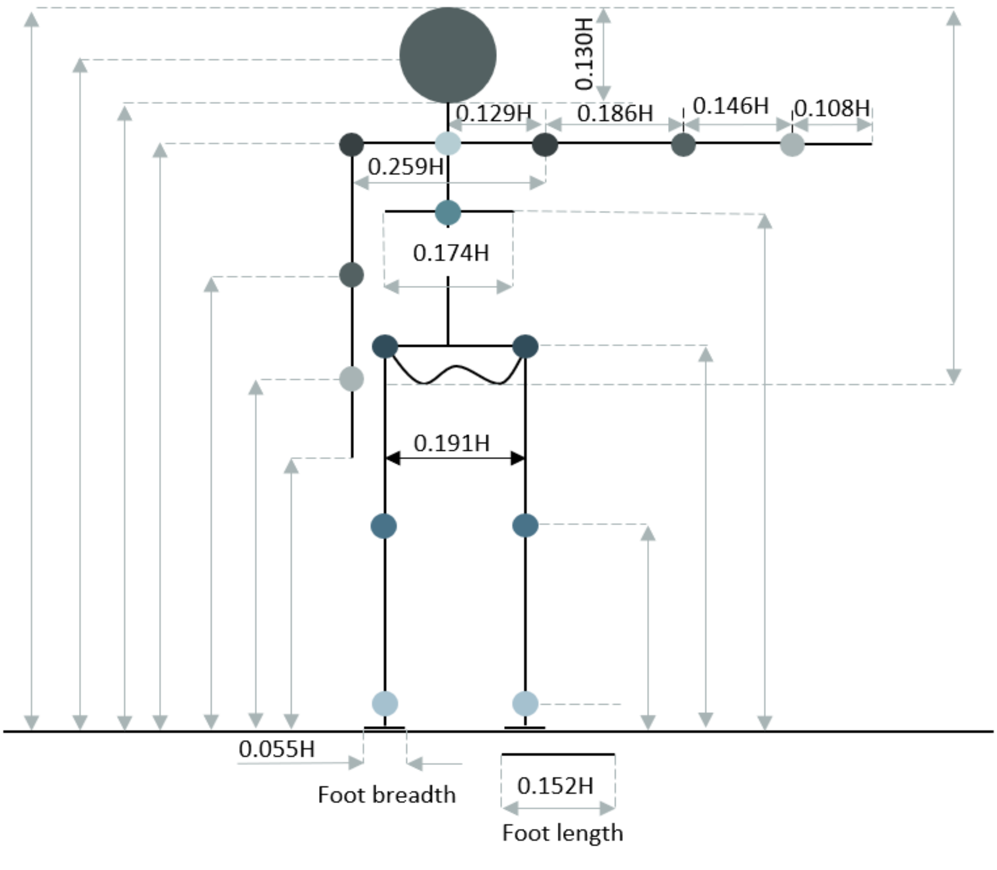

Figure 8 Position of the center of mass (Drillis and Contini, 1966)

5.4 Moment of Inertia

The next step is to determine the inertial effects of the bodies. Each of the three rigid bodies has both mass that resists linear acceleration and an inertia that resists rotational acceleration. The size of inertia depends on the distribution of the body mass with respect to the axis of rotation. The points of a body with greater mass and located further from the axis have a greater moment of inertia. (McCaw, 2014)

6 HEAD INJURIES CAUSED BY A FALL

A head injury is any injury to the brain, skull or scalp. It does not matter if it is a bruise, a mild concussion or a traumatic brain injury (TBI). The consequences of an injury vary greatly depending on what caused the head injury and how serious the injury is. According to the statistics shown in Figure 9, falls are among the most common causes leading to TBI. Unfortunately, the falls were no more specified in the statistics article.

In general, falls can be classified into three basic groups - falling from standing on a mat, falling from a height and free-falling. The main difference between the individual types is the height from which the fall occurs. A typical example of a fall on a mat is a common fall backwards. In this case, the muscles do not keep the head in a safe position and when the body comes into a contact with the mat, the head is struck by a large dynamic force. The same is valid for falls from a height, when the body flips over the edge of a structure and then moves in a uniformly accelerated motion, which is also accelerated by gravitational force. The air resistance is negligible in this case. In the case of free-fall, there is an accelerated movement, and when the resistance equals the force of gravity, the person begins to move at a constant speed. (Straus, 2001)

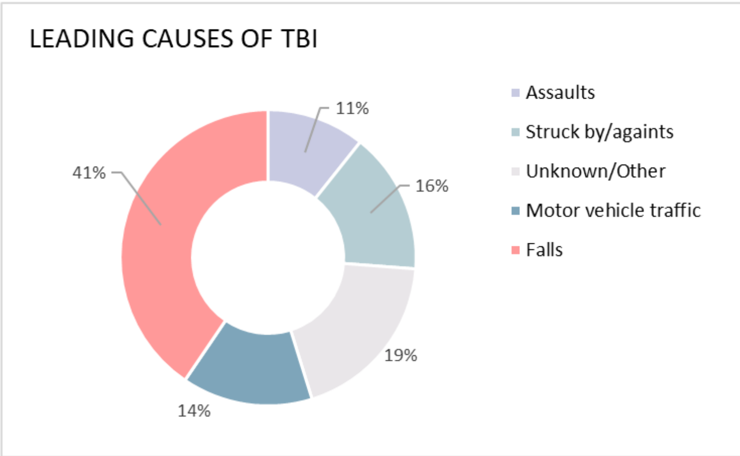

Figure 9 Traumatic Brian Injury (Schmitt, et al., 2007)

In addition to height, which has a major impact on the injury, there are other physical factors to consider. The actual anatomy of the head, the type of collision and the mechanism of the brain injury play a key role in the development of the brain injury. The individual terms are introduced and explained in this chapter.

6.1 Anatomy of the Head

The human head (*cranium*) is a very complex structure that consists of several layers. The outer layer is the scalp, followed by the skull, meninges and central nervous system. The scalp is about 5-7 mm thick layer of skin which is usually covered with hair subcutaneous connective tissue and muscles and fascial layers. When tensile force is applied, all layers move together as one. Below that is the connective tissue and periosteum (i.e. the fibrous membrane) that covers the bone skull. (Schmitt, et al., 2007)

6.1.1 Skull

The skull is generally divided into two parts - the *neurocranium* and the *splanchnocranium*. The bones of the neurocranium surround the brain and their basic function is to protect the brain. Some of the bones also protect the sensory organs. The bones of the neurocranium include -*os occipitale*, *os phenoidale, os ethmoide, os temporale, os frontale, os parientale, os lacrimale, os nasale* and *vomer.* The bones of the splanchnocrania form the facial part and some of them are also part of the functional masticatory apparatus. Splanchnocranium consists of *maxilla, palatinum os, zygomaticum os, hyoideum os, ossicula auditus*. (Čihák, 2011)

The adult skull consists of number of skull bones, which are connected by *sutures lines*, i.e., solid fibrous connections (Figure 10). The only bone of the face that is connected to the skull by freely moving joints is the mandibula. The thickness and curvature of individual bones can vary considerably. (Schmitt, et al., 2007)

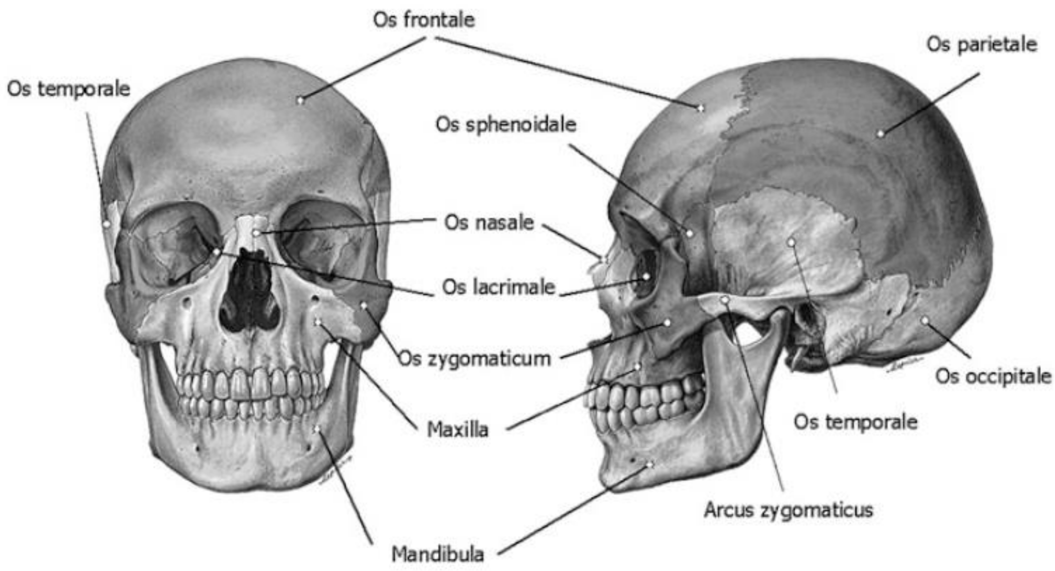

Figure 10 Anatomy of the Head: body structures of the skull (Schmitt, et al., 2007)

6.1.2 Meninges

The envelopes of the brain and thus of the entire CNS form three fibrous layers (Figure 11). The outer layer is formed by a solid fibrous membrane called the Dura mater, followed by a vascular layer of the Arachnoid, and the Pia mater directly connected to the brain. The Dura mater and the *Arachnoidea* are separated by a narrow space called the Subdural Space. By analogy, it separates the Epidural Space by the Arachnoid from the Pia Mater. *Subarachoid* space and the ventricles of the brain are filled with cerebrospinal fluid (CSF), which protects the brain (and spinal cord) from mechanical shock. CSF surrounds the brain from all sides, thus protecting it from shocks, pressure changes and temperatures. (Čihák, 2011)

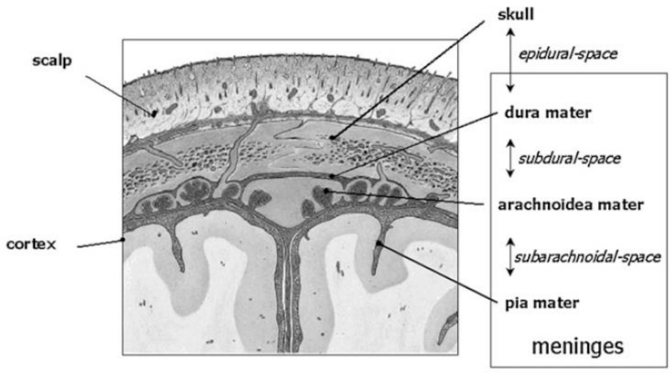

Figure 11 Meninges (Schmitt, et al., 2007)

6.1.3 Brain

The human brain is the most complex organ of the body, which is the controlling and integrating organ of the human nervous system. It directs and controls all bodily functions, as well as all conscious activities. The brain of an adult makes up approximately 2% of human weight. Because of its incompressibility, it is prone to injury. (Čihák, 2011)

6.2 Collision Types

There are many types of mechanisms leading to head injuries. In principle, however, they can only be the result of static or dynamic loading. According to the literature, static load is defined as a load lasting longer than 200ms. Under such load, the head deforms until it reaches the maximum deformation. In the case of falls, dynamic loading is more common. (Schmitt, et al., 2007)

There are two types - **contact** and **non-contact**, each of which results in a different head response. Direct contact of the head with (or without) an object can cause the skull to deform, which can result in a direct fracture (often near the point of impact) or an indirect fracture. Furthermore, local brain injuries (even without fractures) such as epidural hematoma or contusion or scalp injuries are observed after skull deformity. (Schmitt, et al., 2007)

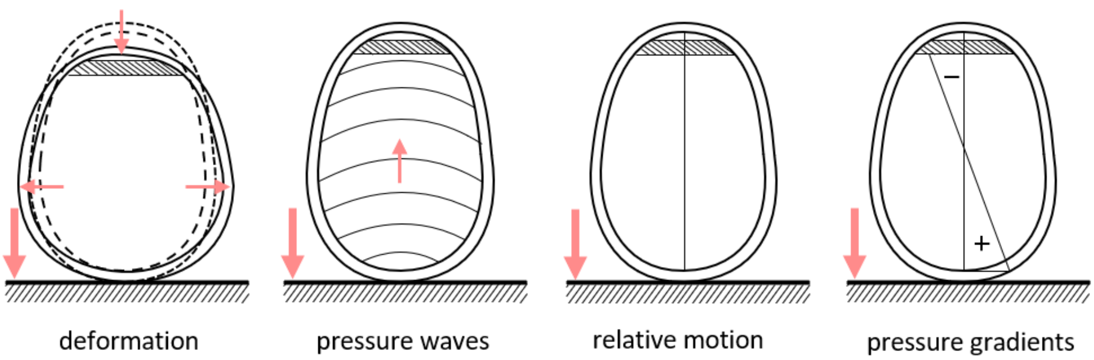

Figure 12 Different injury mechanism for contact impact (adapted from (Vetter, 2000))

In addition, rapid contact load creates stress waves that propagate in the skull or brain. The propagation of waves in the brain can lead to a pressure gradient at the point of impact (*coup*) and a negative pressure at the opposite side of the impact (*contre-coup*). Such a mechanism is designed to create intracranial compressions that cause focal injuries to brain tissue and bruising. Among other things, the pressure gradient can cause shear stress inside the deep structure of the brain. (Schmitt, et al., 2007)

Contact loading can also lead to a relative movement of the brain surface in relation relative to the inner surface of the skull. The consequences can be superficial bruises on the brain and rupture of the bridging veins. (Schmitt, et al., 2007)

In non-contact situations, the head load is exclusively due to inertial forces, i.e., acceleration/deceleration of the head. Acceleration can be translational or rotational. Translational acceleration generally leads to focal brain injury, while rotational acceleration causes diffuse brain injury. (Schmitt, et al., 2007)

6.3 Head Injury Mechanism

The internal mechanical response of individual anatomical parts of the head to external mechanical loads varies considerably. If the external mechanical load exceeds a certain value, called the injury tolerance level, a specific injury occurs. Within this chapter, the individual mechanisms leading to the occurrence of typical injuries will be presented.

6.3.1 Brain injury

The most serious head injuries are considered to be skull and brain injuries, including meninges. However, there is a number of injuries that can occur as a result of an impact during a fall. These are systematically classified in Figure 13. In principle, head injuries are divided into open or closed injuries, depending on whether the Dura mater is injured (open) or not (closed). This chapter will not mention minor injuries that do not endanger life of the individual and cannot cause permanent consequences. (Schmitt, et al., 2007)

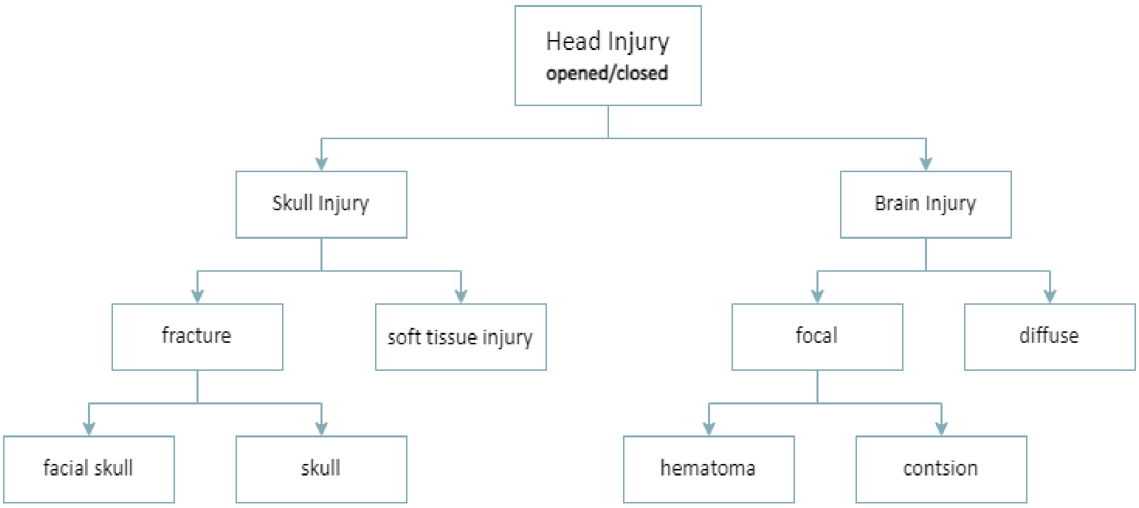

Figure 13 Overview of the Head Injuries (adapted from (Schmitt, et al., 2007))

Brain injuries are classified into two categories - **diffuse injuries** and **focal injuries**. **Diffuse brain injury** is a term that covers a wide range - from mild concussion to diffuse white matter injury. The most common form of this injury is a mild concussion (fully reversible, without loss of consciousness). A more serious form is concussion with loss of consciousness. Whether there will be any long-term effects depends on whether or not there is a brain injury. (Schmitt, et al., 2007)

Focal brain injuries are injuries where the damage is well defined locally. Possible injuries are bruising at the point of impact (*coup contusion*) and the opposite side (*contre-coup contusion*). Regarding the hematoma, three different types according to the place of bleeding are distinguished: epidural hematoma, subdural hematoma and intracerebral hematoma**.** (Vesely, et al., 2012)

Epidural hematoma, i.e., bleeding above the dura mater, is observed due to injuries to the skull and lower meningeal vessels. So it is not caused by a brain injury. This usually involves a fracture of the skull, but it can happen without it. If the hematoma is below the Dura mater, which is called a subdural hematoma. This can be caused by lacerations of the cortical veins and arteries penetrating the wounds, bleeding from large bruises into the subdural space, and rupture of the bridging veins between the surface of the brain and the *Dural sinuses*. The mortality rate of this type of hematoma exceeds 30%. And intracerebral hematomas are defined by homogeneous clusters of blood in the brain. (Schmitt, et al., 2007)

7 CRITERIA OF HEAD INJURIES

It is generally known that injuries are the result of excessive stress and occur when the mechanical tolerance of body structures is exceeded. In the past, a head impact was distinguished as either safe or dangerous. However, such division was not sufficient to objectively assess the severity of the injury. Therefore, criteria were developed for evaluating the severity of the injuries, i.e., for evaluating the mechanical parameters that led to the injury, and at the same time it was possible to measure them in some way.

Such measurements were performed in various ways – whether they were crash tests of mannequins and corpses, then animal experiments or using numerical models. The concept of injury severity scale was adopted, and this scale was correlated with the measured parameters. Currently, one of the most used parameters is the time history parameter of the linear acceleration of the center of mass, on which the later criteria for evaluating the severity of injuries are based. (Simms, et al., 2009)

The criteria can be used to evaluate injuries to all parts of the body; however, they are most often used to evaluate dominant head injuries. This is one of the most serious injuries that can occur. However, before any criteria are applied, it should be remembered that they also have their limits. Whether it is the sample size, the age of the (dead) subjects, or scaling of animal tests for humans. In short, everything introduces a certain mistake into the criteria, which cannot be neglected. Therefore, the criteria should be applied to individual cases with great caution and should serve to predict the likelihood of an injury rather than unambiguously stating the occurrence / non-occurrence of an injury.

7.1 Gadd Severity Index (GSI)

The Gadd Severity Index was first described by Charles Gadd in 1966 for use in the automotive industry. Due to the correlation of injury severity with time and deceleration on impact, a relatively simple formula was derived:

$$\mathrm{GSI} = \int_{t_0}^{t} \boldsymbol{a}(t)^{2.5} dt, \tag{44}$$

where$\boldsymbol{a}(t)$ is a linear acceleration, 2.5 is a weighting factor based on the Wayne State Tolerance Curve, and the limits of integration t, t_0 are the times at the onset and end of the impact, respectively. Based on the collected data, the threshold value is considered to be 1 000. (Hong, 2014)

7.2 Head Injury Criterion (HIC)

Versace (1971) performed some improvements to the GSI based on data from the automotive industry. Although both GSI and HIC include time in predicting the injury, the improved Head Injury Criterion has been supplemented with specific time ranges:

$$\mathrm{HIC}_{15} = max\left\{(\mathrm{t}-\mathrm{t}_0)\left[\frac{1}{(\mathrm{t}-\mathrm{t}_0)}\int_{\mathrm{t}_0}^{\mathrm{t}}\boldsymbol{a}(\mathrm{t})dt\right]^{2.5}\right\}, \text{where } (t-t_0) \le 15\, ms \qquad (45)$$

where $\boldsymbol{a}(t)$ is the resultant acceleration expressed as a multiple of the acceleration of gravity (g), t and t_0 are any two points in the time during the period of the head impact which are separated by not more than a 15-millisecond time interval selected to maximize HIC and 2.5 is a weighting factor based on the Wayne State Tolerance Curve. The threshold for the HIC is set at 1 000 with different time intervals. For the criterion $\mathrm{HIC}_{36}$is time interval 36 milliseconds. (Hong, 2014) The threshold values of the HIC criteria vary for different genders and age groups. Their values are given in Table 5.

Table 5 Threshold values for HIC (Eppinger, et al., 1999)

	Male	Female	6 year	3 year	12 Month
HIC_{15}	700	700	700	570	390
HIC_{36}	1000	1000	1000	900	660

The relationship between the HIC rate and the probability of a fracture is shown in Figure 14. From the dependence plotted in this way, it can be easily determined that for the threshold value $HIC_{36} = 1000$, there is a probability up to 50% of a skull fracture.

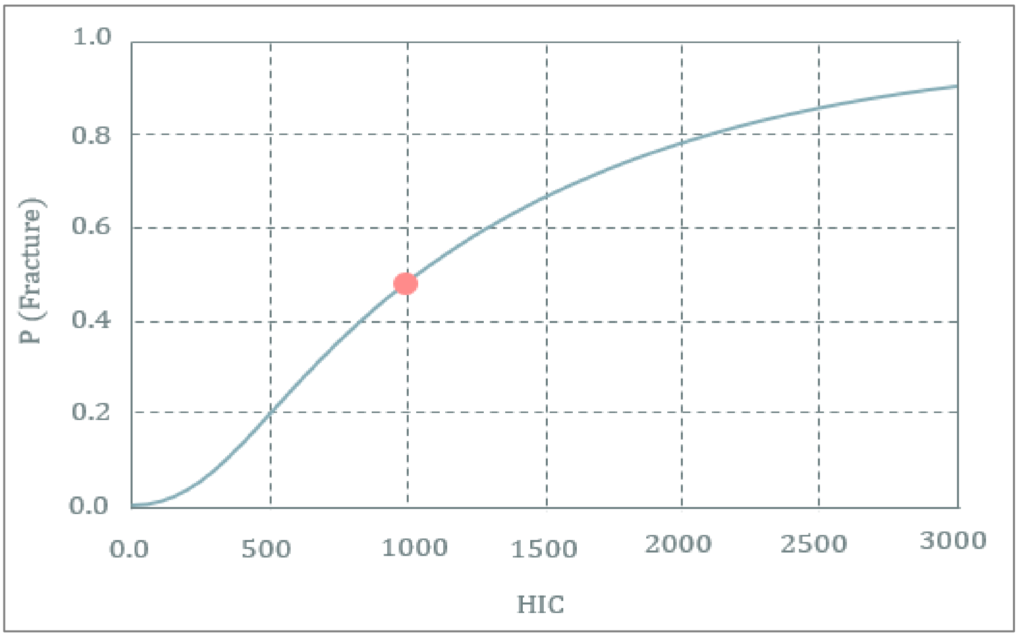

Figure 14 Relationship between HIC and skull fracture probability [%] (Dionne, et al., 1997); (Mackay, 2007)

Although this criterion is suitable for predicting the probability of a skull fracture, its use is very limited. The reason is that the criterion only considers linear acceleration and ignores the effect of rotational acceleration. This fundamentally limits the use of the criterion, as it is not possible to predict whether and to what extent a brain injury will occur.

7.3 Abbreviated Injury Scale (AIS)

In 1971, the Abbreviated Injury Scale was defined, where the original intention was to map a series of anatomically defined injuries by several parameters (energy dissipation, permanent impairment, treatment period). In the following years, this criterion was improved and today consists of a list of approximately 500 injuries and injury levels from 1 (minimum injury) to 6 (virtually non-survivable injury) (Gennarelli, et al., 2008). Table 6 below shows severity levels with a brief definition.

Table 6 Abbreviated Injury Scale (AIS) (Shojaati, 2003); (Mariotti, et al., 2019)

AIS	Injury level	Description of possible injuries
1	Minor	Light brain injuries with headache, vertigo, no loss consciousness, light cervical injuries, whiplash, abrasion
2	Moderate	Concussion with or without skull fracture, less than 15 minutes of unconsciousness, corneal abrasions, detached retina, face or nose fractures
3	Serious	Concussion with or without skull fracture, more than 15 minutes of unconsciousness without severe neurological damages, closed or depressed skull fracture without unconsciousness or other injury indications in skull, loss of vision, open face bone fracture with antral or orbital implications, cervical fracture without damage to the spinal cord
4	Severe	Closed or impressed skull fracture with severe neurological injuries
5	Critical	Concussion with or without skull fracture with more than 12 hours of unconsciousness with hemorrhage in skull and/or critical neurological indications
6	Currently untreatable	Death, partial or full damage to brainstem or the upper part of cervical due to pressure or disruption, fracture with injuries to the spinal cord

Table 7 is its extended version, which also shows the values of the maximum linear load and a column indicating the percentage of deaths.

Table 7 Extended table about Abbreviated Injury Scale (Wilde, et al., 2019)

AIS	Injury Level	Fatality Range	Max linear acceleration
1	Minor	0.0%	50 – 100 g
2	Moderate	0.1 – 0.4 %	100 – 150 g
3	Serious	0.8 – 2.1 %	150 – 200 g
4	Severe	7.9 – 10.6 %	200 – 250 g
5	Critical	53.1 – 58.4 %	250 – 300 g
6	Currently untreatable	Virtually non-survivable	> 300 g

7.4 Correlation between HIC and AIS criterion

Based on many post-mortem experiments with (dead) bodies, a correlation was made between the HIC and the AIS criterion. Table 8 was obtained from the experiments and the subsequent correlation of the parameters. The dependence of the criteria is plotted in Figure 15.

Table 8 Correlation between HIC (Wilde, et al., 2019) and AIS (Gennarelli, et al., 2008)

HIC	AIS	Head Injury
135 – 519	1	Headache or dizziness
520 - 899	2	Unconscious less than 1 h, linear fracture
900 – 1254	3	Unconscious 1 – 6 h, depressed fracture
1255 – 1574	4	Unconscious 6 – 24h, open fracture
1575 – 1859	5	Unconscious more than 24 h, large hematoma
> 1860	6	Nonsurvivable

7.5 Relationship between the Probability of a Head Injury and the HIC

Prasad and Mertz presented a relationship between the probability of developing head injuries of varying severity and HIC. Its graphic subdivision is given on Figure 15.

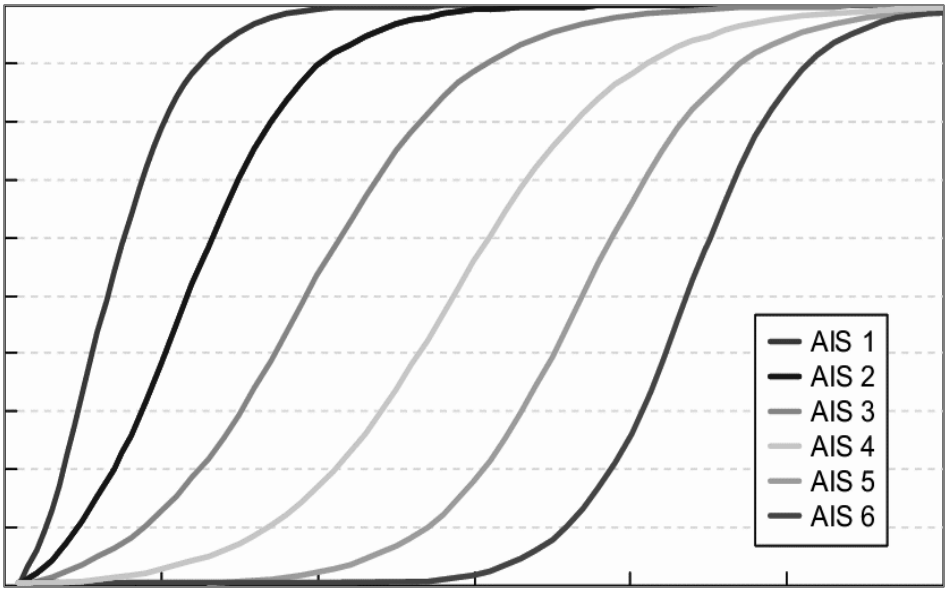

Figure 15 Probability of head injuries of different severities for given HIC values (Hayes, et al., 2007)

According to the literature (Prasad, et al., 1985), these curves can be defined using an exponential model described by the formula:

$$\Pr(\text{AIS}) = 1 - e^{(-a \cdot \text{HIC}^{b})} \tag{46}$$

Table 9 contains values of coefficients that were determined by the authors based on the relationship between probability and HIC values, which were presented in the literature (Mackay, 2007); (Prasad, et al., 1985)

Table 9 Coefficients values of the proposed exponential model (Prasad, et al., 1985)

Tissue Damage	a	b
Minor (AIS 1)	$8.79 \cdot 10^{-6}$	1.94
Moderate (AIS 2)	$4.18 \cdot 10^{-7}$	2.24
Serious (AIS 3)	$9.00 \cdot 10^{-9}$	2.64
Severe (AIS 4)	$2.30 \cdot 10^{-9}$	2.69
Critical (AIS 5)	$2.23 \cdot 10^{-19}$	5.66
Usually fatal (AIS 6)	$4.76 \cdot 10^{-31}$	9.03

8 CUSTOM SOLUTION

In this chapter it will be introduced the method used for the creation of the physical world, and the steps in making a simplified 2D mechanical model of the human body, where weight and height are the only parameters. The model is made up of several segments, which represents a human body by their shapes and characteristics. The segments are connected with each other by joints. A simulation of a fall is done by applying force to a certain area. Based on the values obtained from this simulation, the criteria for determining the probability of head injury were evaluated.

8.1 Programming Language Python

First it was necessary to decide in which software the simulation will be created. The selection was limited to two well-known software - OpenSim and Matlab with Simulink. The first one is an open source OpenSim software, which allows users to view, edit and analyze muscle-skeletal models. The software can be used to model motion and calculate inverse kinematics and dynamics. However, its disadvantage is the inability to apply force to a specific place. For this reason, this software was not selected. Another option considered was Matlab with Simulink. Matlab is a programming environment (with its own programming language), which specializes in scientific and technical calculations and modeling. Its extension is Simulink, which is a program suitable for creating simulations and modeling of dynamic systems. Although Matlab seemed like a good choice, its disadvantage is the need for a license. Therefore, the resulting solution would not be available to everyone.

Therefore, another alternative was sought. In the end, the Python programming language was chosen, which is accessible to everyone, easy for beginners to learn, and also allows the use of many open-source libraries. Their advantage will be presented later.

8.2 Creation of the Project

To find a solution, the programming language Python was chosen. The project was written in Visual Studio Code IDE (Integrated Development Environment). It is a source-code editor made by Microsoft for Windows, Linux and macOS. It is a streamlined code editor with support for development operations, like debugging and version control. The open-source libraries used will be described later. They were used for the definition of the physical world, creating of the model, the simulation run and the data evaluation.

8.3 Physical World

The aim of numerical simulation is to obtain results, which are as close to reality as possible. To achieve that, it is necessary to create the most realistic world possible, in which the simulation will run. Using the defined function of libraries a blank screen with the physical world was created, in which the simulation later took place.

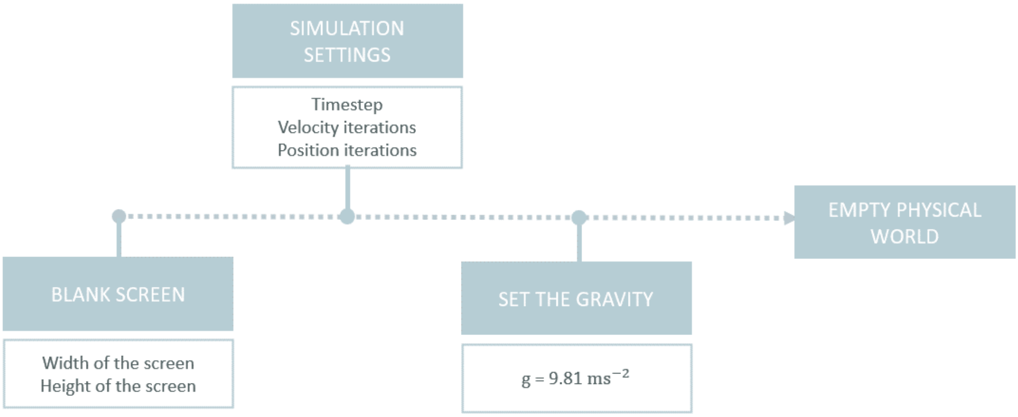

Figure 16 The scheme of creating the physical world

8.3.1 The Pygame Library

The Pygame library is a package of modules created for development of computer games and simulations. These modules offer functions, which make simulations easier. The basic structure of the Pygame library uses two modules – *pygame.display* and *pygame.event*. The first of these modules is used to create a simple window without any controls, into which graphic features can be drawn later. Then there is an infinite programmed loop in which the whole content of the event queue is being read repeatedly. This reacts to the type of event QUIT, which suggests that the whole application should finish.

To avoid unpleasant flickering when drawing the game scene, the Pygame library uses so called *double buffering*, where the graphical user interface of the application is not performed directly onto the screen, but instead onto a separate subsidiary bitmap known as *back buffer*. The main reason is for the user not to see unpleasant flickering when deleting/drawing of the background.

Once all graphical objects are drawn into back buffer, it is then necessary to make this buffer visible. In this case, the role of the front and the back buffer are simply swapped using *pygame.display.flip*.

The operation of the simulation is based on the fact that the world is simulated in **discrete time steps**. This means that the world is updated at each time step depending on its selected value. As a rule, the time step FPS = 1/60 s is used, which is a sufficient value for creating games. However, greater accuracy is required for this particular simulation, and therefore FPS = 1/200 was chosen. The whole rendering process is started iteratively, with smoothness provided by the *pygame.time.Clock* object, which slows down the run according to the set time step (FPS) in case the speed is too high so that the graphic output is smooth.

8.3.2 The Box2D Library

Box2D Library is a free open source 2-dimensional physics simulator engine. The Box2D library contains an object called World, which represents the entire scene. Two basic parameters are needed to create a physical world. The first is to set the value of the gravitational force that acts on all dynamic bodies. The second parameter is whether the objects can sleep or not. This parameter determines whether bodies are allowed to sleep if nothing is done. This means that they are excluded from the simulation until something "wakes them up" again (collisions with another body, acting force, etc.) (Feronato, 2012)

It is already known that it is necessary to select a simulation time step that determines how often the step is called. Since the number of steps per second also affects the bodies and their reactions to the gravitational force, it is still necessary to define the iteration value for speed and position. (Feronato, 2012)

It is important to note here that whilst the Pygame library works with pixels, Box2D works in meters and with angles in radians. Also the beginnings of coordinates have different libraries defined differently, so it is therefore useful to create a certain conversion link.

8.4 2D Human Body Model

In the next step, it was necessary to create a 2D mechanical model of the human body, which would be as close as possible to the actual behavior of the human body. In order to achieve this goal, its geometry had to correspond to the human body as well as its parameters. The whole model was designed based on two input parameters - weight [kg] and height [cm] of the individual. All other necessary parameters were calculated thanks to these two parameters and on the basis of the relations given in Chapter 5. The scheme according to which it was followed is shown in Figure 17.

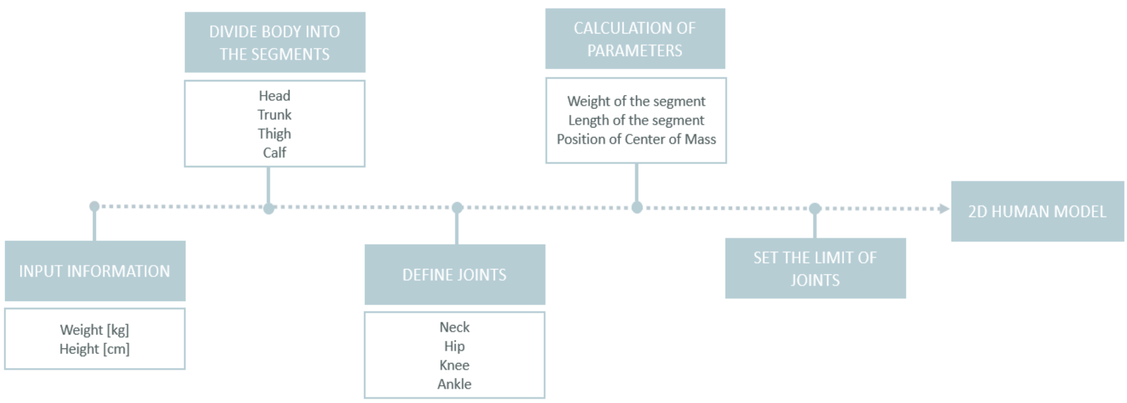

Figure 17 Scheme of creating a 2D Human Model

8.4.1 Geometry Model

For this simulation, it was necessary to design a model of the human body. The aim was to make the model as realistic as possible, but not too complicated. Therefore, a model was designed that consisted of four main elements and three joints between them. Due to their parameters (weight, size) the following segments were considered - calf, thigh, trunk and head. These were connected by joints - knee, hip and neck. Figure 18 shows how the body was divided into segments.

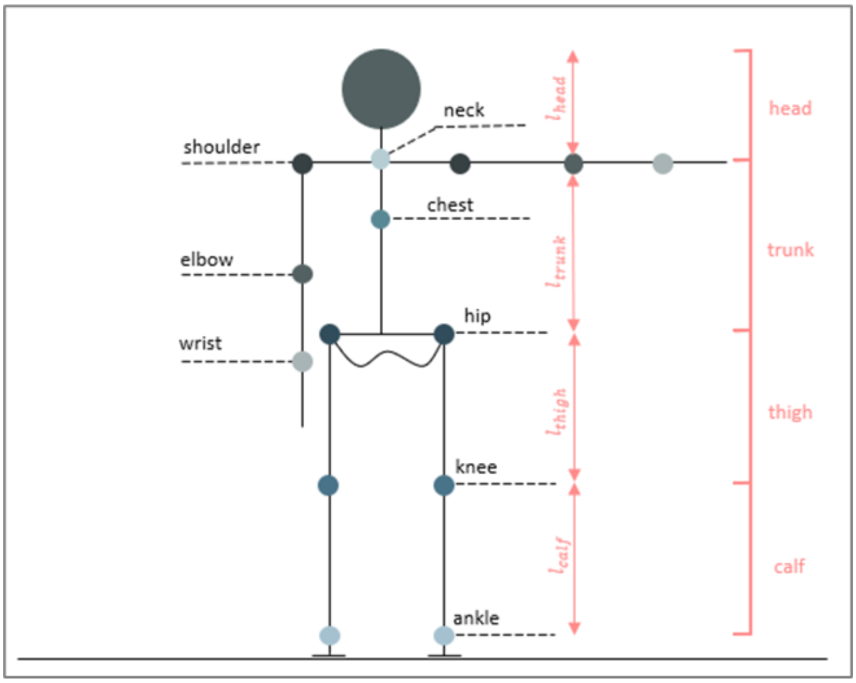

Figure 18 Designed model of the human body

The segments had to be further specified, not only by their material parameters, but also by the appropriate geometric shape. The material parameters of the segments were determined on the basis of the input parameters, as mentioned in the introduction of the chapter. As for the geometric shapes of the segments, several were tested during the creation of the model. In the end, it turned out to be the most suitable to use a sphere shape for the head body and an ellipse shape for the other segments. The problem with other shapes arose during the simulation, when unrealistic body positions occurred due to body collisions. This problem was solved by choosing the appropriate segment geometry.

8.4.2 Creating a Model

The human body model was created using the Box2D library. It defines as a body basically anything that it can move with or interact with. There was nothing more needed for this model, so this library was a good choice. As part of this step, a model was created from individual bodies that responded to gravitational forces, as well as a ground body representing the impact surface. Subsequently, the individual bodies were joined by means of joints.

The Box2D library allows, as in the real world, the creation of different types of bodies - static, kinematic and dynamic. The first term mentioned is a static body that does not respond to any force, impulse or collision, nor does it move. The Box2D library considers each body to be static by default. The complete opposite is a dynamic body that responds to all forces, impulses and collisions. Although it is possible to move dynamic bodies manually, it is recommended to let them move due to world forces or the impact of other bodies. The hybrid between a static and a dynamic body is a kinematic body. Such a body does not respond to forces but can be moved in the scene. Kinematic bodies do not collide with other static or kinematic bodies. (Feronato, 2012)

When creating a *body*, it is necessary to attach the appropriate *fixture* to the points. This allows you to define the shape of the bodies, but also to define its various material properties using density, the value of the coefficient of friction and the restitution coefficient. The density value affects the weight of the body and cannot be negative. The coefficient of friction takes values from 0 (no friction) to 1 (maximum friction). The coefficient of restitution determines how much the body bounces off after a collision - 0 (inelastic collision) to 1 (perfectly elastic collision) and its value cannot be negative. (Feronato, 2012)

Due to the possibilities of the library and the requirement that the bodies correspond as much as possible to real parts of the human body, the segments were defined as dynamic bodies. Furthermore, they were assigned the appropriate shapes and locations in the physical world. A body representing the impact surface was created in a similar way, with the only difference that it was considered a static body.

The creation of the whole human body was possible by interconnecting dynamic bodies using joints. The result was a reduction in the mobility of individual bodies and thus a reduction in the number of degrees of freedom. Although the library's offer is wide in terms of joint types, the Revolute joint type was chosen for all created joints. It is a rotating joint that has one degree of freedom - rotation around the anchor point. When defining individual joints, in addition to the type and position, the lower and upper limits were set, limiting the range of motion of the connected bodies, as is the case in the real world. (Feronato, 2012)

8.5 Applied Forces and Impulses

The created physical world made it possible to create realistic simulations by applying forces and impulses. During the simulation, the bodies were continuously affected by gravitational force and their movement could be further influenced by the action of forces and impulses. In the case of this simulation, a force representing the force of the blow was applied. In addition to its size, it was also necessary to set the direction and the place in which it worked. In addition, if the force did not act on the center of the body, torque was created which affected the angular velocity. The impulse was not applied, but if it did, the velocity of the body would change immediately.

8.6 Collisions

In the previous steps, a physical world was created in which the body and the ground and model of the human body were placed. The human body was affected not only by gravity, but also by a certain force representing a blow. Depending on its size, the body could deviate from the equilibrium position and then fall on the ground, i.e. the bodies collided. Figure 19 shows what the simulation looked like before and after startup.

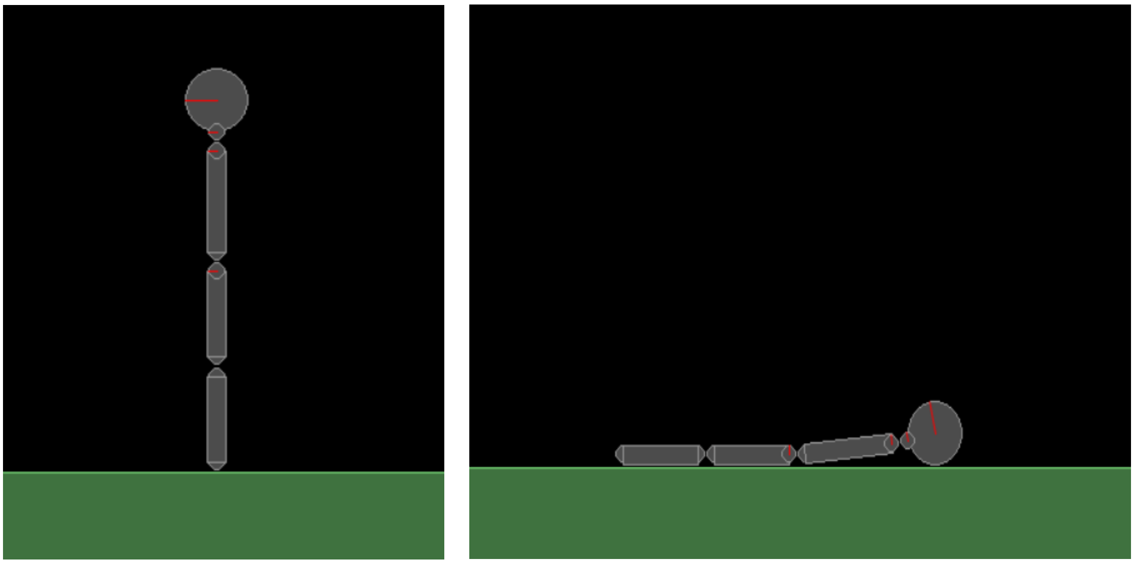

Figure 19 Simulation of a fall performed in Visual Studio Code

It is generally known that if two bodies collide, a contact point can always be found there. The Box2D library has a defined Collision module, which stores information about which bodies collided. All stored information can be found using *b2ContactListener,* which works with collisions in several phases - *Beginning*, *End*, *PreSolve* and *PostSolve*.

The contact of the head with the pad was important for this simulation. By a relatively simple modification of the functions listed in *b2ContactListener*, the moment when the bodies began to touch and stopped was found. Furthermore, the *PostSolve* function was modified, which provided, among other things, information about the impulse at the point of contact.

8.7 Analysis of the Obtained Data

The velocity, acceleration and impact force were recorded during the impact. These values were then used to evaluate the HIC value. Based on the calculated value, the probability of injury was calculated. All worked values were stored in a CSV file and are listed in Appendix A. The values given in Appendix A are divided into three main parts. The first part consists of the defined initial conditions of the simulation, the second part shows the values found in the primary impact of the head on the surface and the last part is the calculated values based on the values found. At the same time, the values are divided into two tables, which represent a fall forwards and a fall backwards. The type of fall can be determined based on the direction of the initial force.

9 SIMULATION RESULTS AND DISCUSSION

From the numerical simulation of the fall of the human body, the values of velocity, acceleration and force at the contact of the head with the pad were determined. Furthermore, the behavior of the model was observed when different forces were applied to different parts of the body. In addition, the effect of the pad on impact was also observed. The obtained values were subsequently analyzed and plotted in the following graphs. The data obtained from the numerical simulations used for the processing of this chapter are given in Appendix A.

Before the resulting values from the simulations are presented, it is necessary to state that countless variations of falls can be performed and therefore it is not in the power of the author to perform all possible measurements. Therefore, for simplicity, two cases were considered - fall forward and fall backward. In both cases, the falls were caused by a force between 0 and 3 500 N, which was always applied to the center of gravity of the head. In addition, three types of impact surfaces were considered, which represented an elastic, partially elastic and inelastic surface. The simulations were tested on two people, whose parameters represented the average woman and the average man.

9.1 The Resulting Values of Velocity, Acceleration and Impact Force

The first goal of the simulation was to determine the resulting values of velocity, acceleration and force when the head hit the ground. Appendix A lists all the resulting observed values and therefore it does not make sense to report them individually here. For this reason, one specific situation was chosen for which the results were presented. A fall backward and forward on the partically elastic surface was considered. The values recorded are given in Table 10 and Table 11. It is evident fro the result that although the head velocity at impact for women and men differs, the difference is not large.

Table 10 Fall forwards for a partially elastic surface

WOMAN				MAN		
Velocity $[m \cdot s^{-1}]$	Acceleration $[m \cdot s^{-2}]$	Impact force $[N]$		Velocity $[m \cdot s^{-1}]$	Acceleration $[m \cdot s^{-2}]$	Impact force $[N]$
4.7	935.9	4 349		5.0	1004.0	5 245
4.7	937.5	4 357		5.0	1006.3	5 257
5.0	1003.6	4 664		5.1	1015.5	5 305
5.0	1005.3	4 672		5.6	1125.8	5 881
5.5	1101.4	5 118		5.8	1163.5	6 078
5.5	1105.7	5 139		5.9	1189.4	6 214
5.6	1121.7	5 213		6.0	1195.9	6 248

Table 11 Fall backwards for a partially elastic surface

WOMAN				MAN		
Velocity $[m \cdot s^{-1}]$	Acceleration $[m \cdot s^{-2}]$	Impact force $[N]$		Velocity $[m \cdot s^{-1}]$	Acceleration $[m \cdot s^{-2}]$	Impact force $[N]$
4.1	819.9	3810		4.1	815.1	4258
4.1	822.5	3822		4.3	864.9	4518
4.2	847.0	3936		4.4	871.0	4550
4.3	860.7	4000		4.5	906.7	4737
4.4	885.4	4115		4.6	919.3	4803
4.5	900.2	4184		4.7	936.4	4892
4.6	911.7	4237		4.8	956	4995

It is important to note that although the table shows the same speeds but different acceleration values for some cases, this is not an error. This difference is due to the rounding of numbers.

9.2 Dependence of the Value of the HIC on the Size of the Initial Force

This part deals with obtaining the dependence of the value of the head injury criterion on the initial forces. In order to determine this dependence, it was first necessary to calculate a maximum HIC value. This was achieved by determining the force at the time of the head's impact on the surface. Based on this, a linear acceleration was determined. This was subsequently divided by the value of the gravitational acceleration. Only the value of linear acceleration adjusted in this way could be substituted into the formula (45) and the HIC value could be calculated.

Due to the fact that the impact force is influenced by the surface properties, the simulation was performed for all three types of surfaces. Furthermore, both cases of fall were also simulated, ie fall forward and backward. The dependence found is plotted in the Figures 20 - 25 below. Figures 20 - 22 show the values found for fall backwards and Figures 23 - 25 for fall forwards. In both cases, columns representing the values found for women and men are displayed.

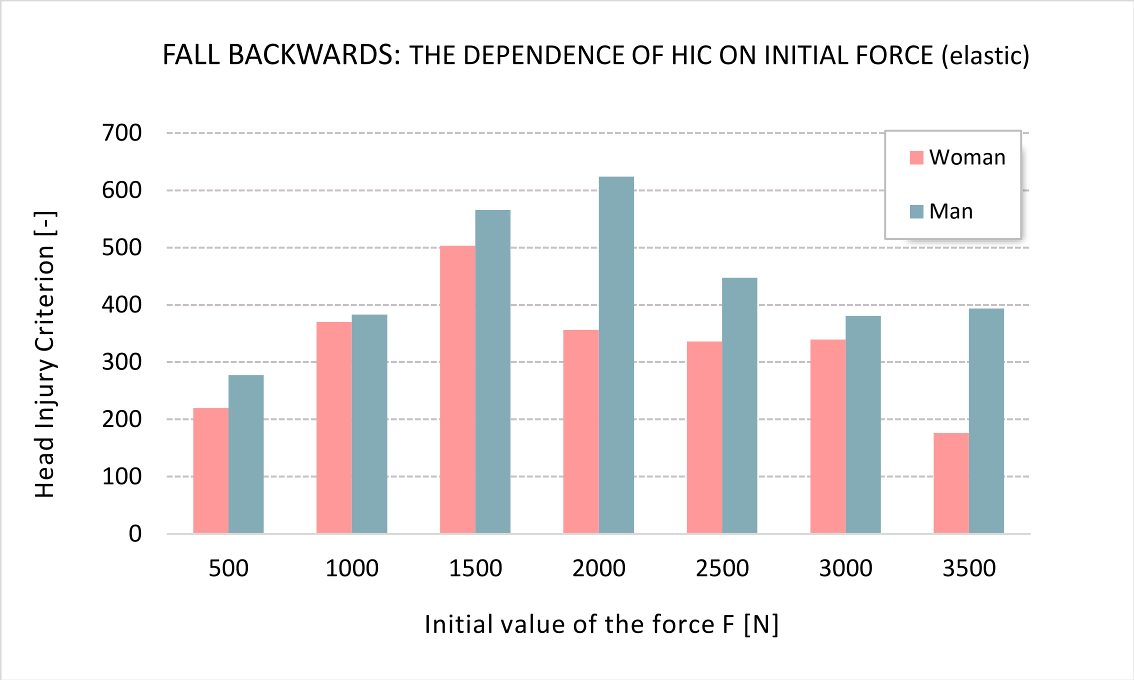

Figure 20 Fall backwards: The dependence of HIC on initial force (elastic surface)

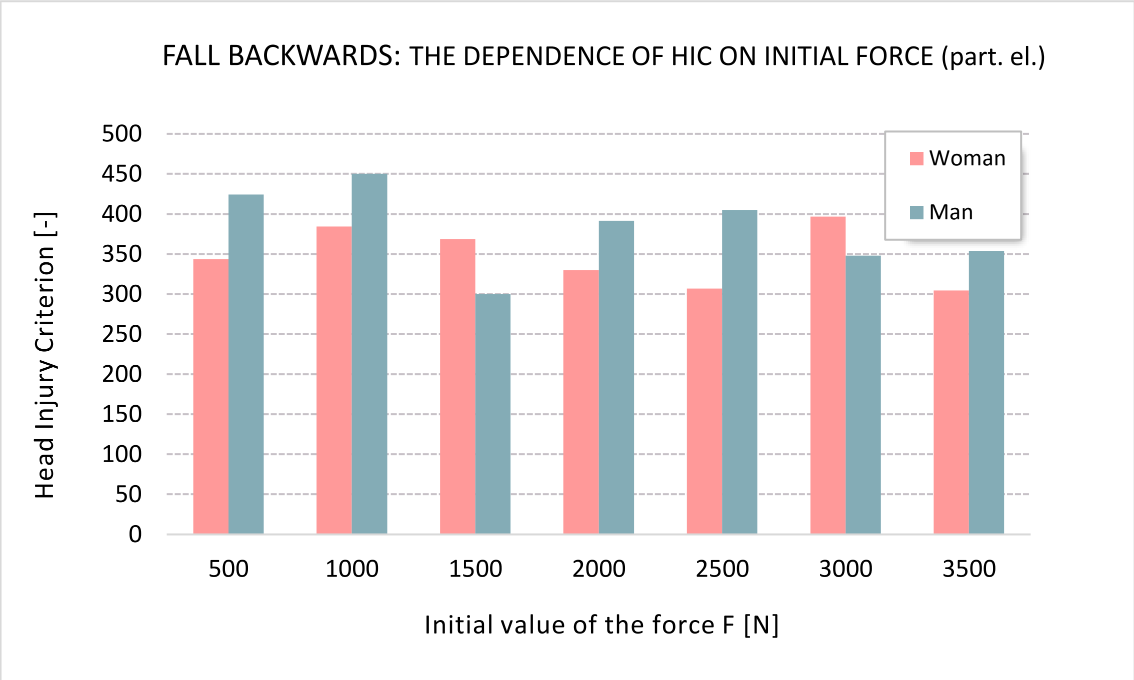

Figure 21 Fall backwards: The dependence of HIC on initial force (part. el. surface)

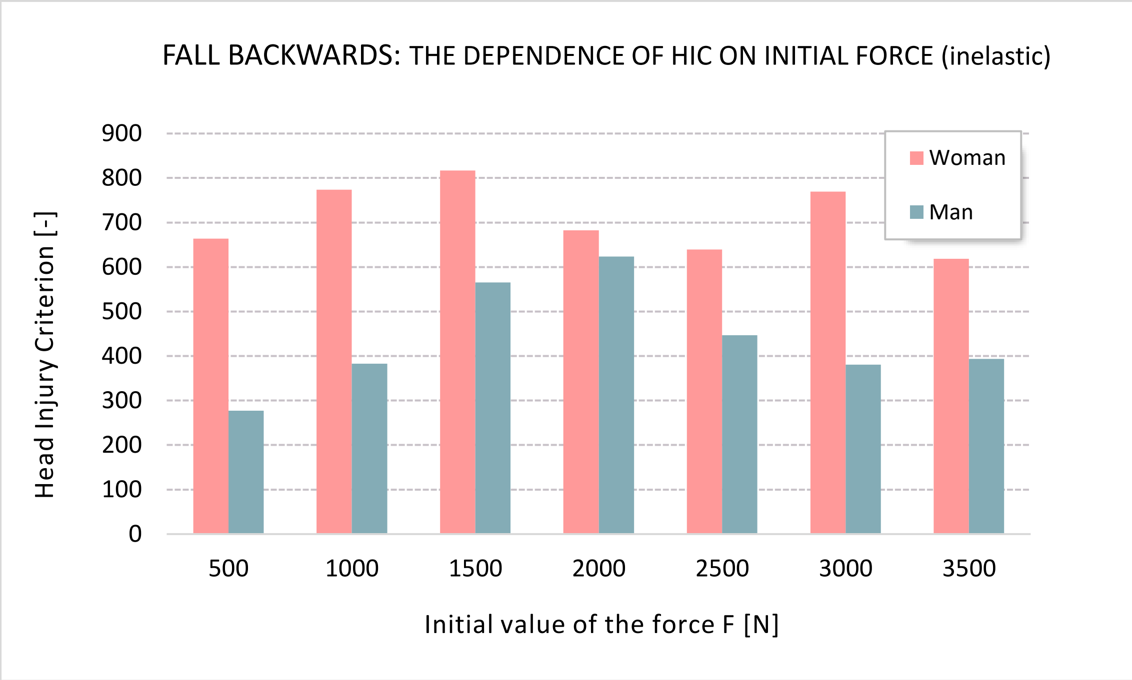

Figure 22 Fall backwards: The dependence of HIC on initial force (inelastic surface)

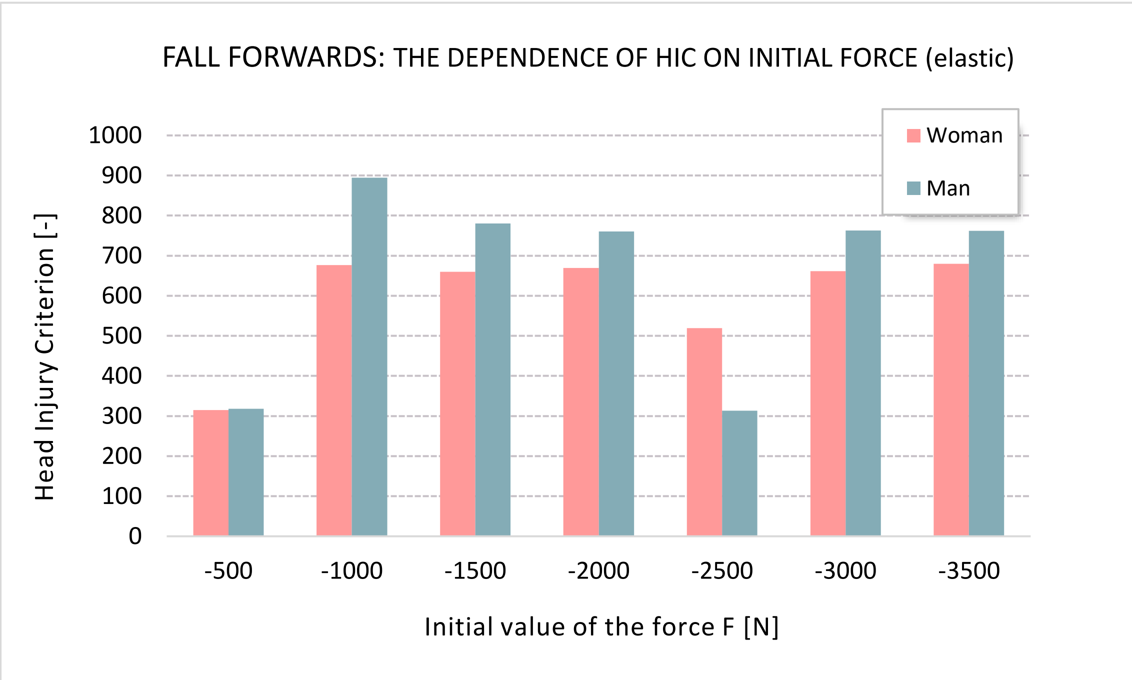

Figure 23 Fall forwards: The dependence of HIC on initial force (elastic surface)

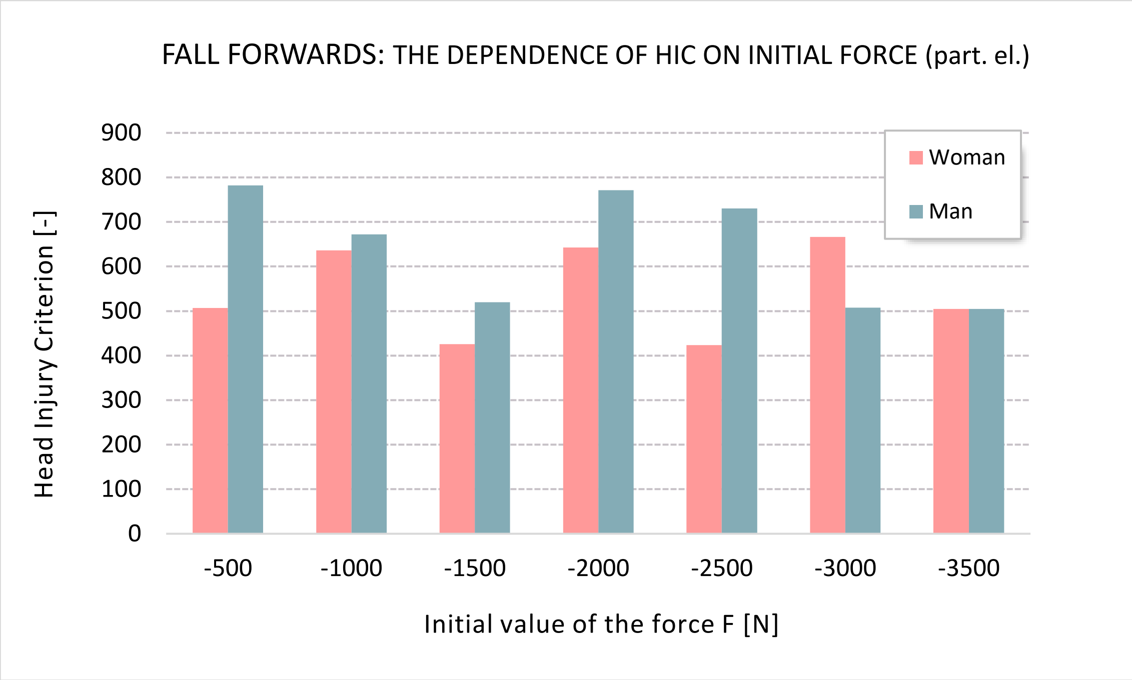

Figure 24 Fall forwards: The dependence of HIC on initial force (part. el. surface)

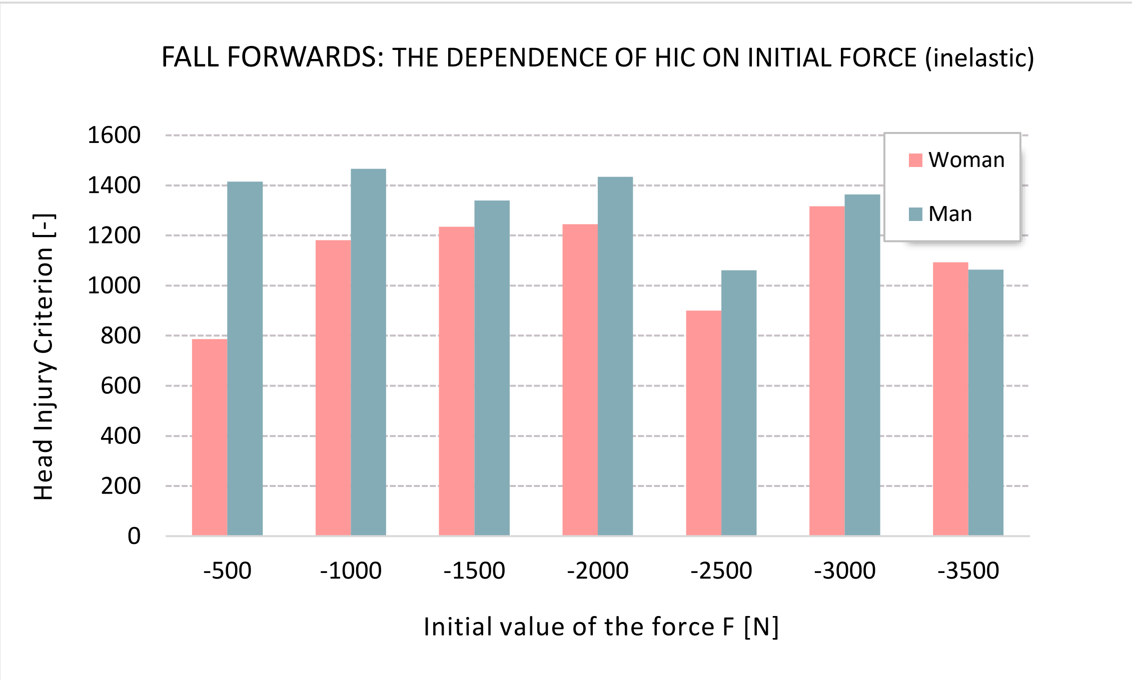

Figure 25 Fall forwards: The dependence of HIC on initial force (inelastic surface)

By comparing the graphs, it was found that the HIC values for falling forward and backward are different. This result is due to the different kinematics of body movement during a fall. The graphs also confirm the logical assumption that a fall to an inelastic surface is likely to cause more serious injuries than a fall to an elastic surface.

9.3 Probability of Injury Based on HIC

The main goal was to determine the probability of injury on impact. Based on the calculated HIC values, it was possible to determine the probability of injury using relationship (46). Using the coefficients in Table 9 the probability for each level of the Abbreviated Injury Scale was determined. The calculation of values is presented on a selected simulation of a fall forwards on a partially elastic surface. Table 12 and Table 13 show the calculated values separately for women and separately for men.

Table 12 Fall forwards for a partially elastic surface (Woman)

HIC [−]	AIS 1 [%]	AIS 2 [%]	AIS 3 [%]	AIS 4 [%]	AIS 5 [%]	AIS 6 [%]
424	66	27	7	2	0	0
425	66	27	7	2	0	0
504	78	37	11	4	0	0
507	78	38	11	4	0	0
637	91	54	20	7	0	0
643	91	55	20	8	0	0
666	92	58	22	8	0	0

Table 13 Fall forwards for a partially elastic surface (Man)

HIC[−]	AIS 1 [%]	AIS 2 [%]	AIS 3 [%]	AIS 4 [%]	AIS 5 [%]	AIS 6 [%]
505	78	37	11	4	0	0
508	78	38	11	4	0	0
520	80	39	12	4	0	0
672	93	59	23	9	0	0
730	95	66	27	11	0	0
771	97	70	31	12	0	0
782	97	71	32	13	0	0

In this particular case, the maximum level of AIS 4 was reached, and even there the percentage of probability of injury is quite small. Therefore, it can be stated that these simulated falls from would not cause fatal injury or death.

9.4 Discussion

This computer simulation can be considered a very useful tool that can be used in the reconstruction of falls. The simulation can help clarify questions about the mechanism of the falls and help determine the input force and starting position. This can be further enhanced by visualization, which makes it easier to understand the situation even for a person who does not have sufficient biomechanical knowledge. And because the simulation follows only the laws of mechanics, an objective biomechanical analysis can be performed that does not depend on the knowledge of the expert. Undoubtedly, its benefit is that it can be used by any user with minimal knowledge of the Python programming language and minimal programming experience.

A certain disadvantage of this simulation is its simplification. Although the effort was made to create a model that was as realistic as possible, it was still necessary to accept certain simplifications when creating it. The body was divided into several segments and some parts of the body were not considered during the fall (although their weight was, the effect on the fall not). Furthermore, the possibility of an injury or energy absorption was not simulated, and as a result, the multibody system behaved more elastically than in reality.

To determine the accuracy of the created simulation, the values of the impact force were compared with the literature (Pascoletti, et al., 2019). In this paper, the authors addressed a similar problem and present the resulting impact forces from the simulation and from the performed experiment. Although the exact initial conditions are not known, the parameters of the created simulation have been tuned to match their simulated scene as much as possible. From the performed simulation, it was found that the values of the impact force were very similarly as the literature, in which these values are verified experimentally.

Based on this, it can be stated that despite all the accepted simplifications, the model is able to correctly simulate the impact forces. At the same time, the movements of the segments and joints during the fall and when they hit the ground correspond visually to reality. The values obtained during the simulation were then used to calculate the HIC criterion, which was used to calculate the probability of an injury. Here it can be stated that in the future it would be interesting to apply this simulation to a real criminal case and validate the found values of the HIC criteria with the results of findings from medical autopsies.

CONCLUSION

This thesis presents the use of a numerical simulation on a specific case of a forensic application, which is the reconstruction of a fall. A simulation of a simple fall from a stand on a mat was performed. In the first step, the physical world in which the simulation took place was created. Then a dynamic model of the human body and ground was created in the world. The multibody mechanical system of the human body with its parameters tried to get as close as possible to the real values of a human body. Subsequently, forces of different magnitudes representing the strikes were applied. Acceleration values were recorded when the head struck the pad, and these were subsequently evaluated using criteria determining the severity of the injury.

The mechanical model of the human body can be further refined by gradually removing the individual simplifications that were adopted during the creation. In addition, it is also possible to extend the numerical simulation by falling from a height and then apply it to a real criminal case. This would undoubtedly be a good example of how such a numerical simulation can play an important role in forensic investigation. And while it is possible that numerical simulations will not always be able to fully and accurately explain all the facts of a police investigation due to the simplifications adopted, it can be expected to provide objective and quantitative information sufficient to clarify the circumstances of the case.

REFERENCE

Adamec Jiří [et al.] Forensic Biomechanical Analysis of Falls from Height Using Numerical Human Body Models [Article] // J Forensic Sci. - November 2010. - pp. 1615-1623.

Ambrósio Jorge and Kecskementhy, Andres Multibody Dynamics of Biomechanical Models for Human Motion via Optimization [Book Section] // Multibody Dynamics – Computational Methods and Applications / book auth. In J.C. Garcia Orden J.M. Goicolea, J. Cuadrado (Eds.). - London : Dordrecht: Springer, 2007.

Catto Erin Publications/Numerical methods [Online] // Box2D: A 2D physics engine for games. - 2015. - https://box2d.org/files/ErinCatto_NumericalIntegration_GDC2009.pdf.

Čihák Radomír Anatomie 1 [Book]. - Praha : Grada Publishing, 2011. - Vol. 2. - ISBN 80-7169-970-5.

Dionne J.P. and Nerenberg A. Makris Reduction of Blast-Induced Concussive Injury Potential and Correlation With Predicted Blast Impulse [Book]. - Ottawa : Med-Eng Systems Inc., 1997.

Duane Knudson Fundamentals of Biomechanics [Book]. - Chico : Springer, Boston, MA, 2007. - Second : Vol. 1. - ISBN 978-0-387-49312-1.

Eppinger Rolf [et al.] Development of Improved Injury Critera for the Assessment of Advanced Automotive Restraint Systems - II // Research Paper. - United States : National Highway Traffic Safety Administration, 1999.

Feronato Emanuele Box2D for Flash Games // eBook. - Birmingham, UK : Packt Publishing, 2012. - ISBN 978-1-84951-962-5.

Franck Harold and Franck Darren Forensic Biomechanics and Human Injury: Criminal and Civil Applications - An Engineering Approach [Book]. - Boca Raton, Florida : CRC Press, 2016. - 9780367778866.

García de Jalón Javier and Bayo Eduardo Kinematic and Dynamic Simulation of Multibody Systems: The Real-Time Challenge [Book]. - New York, NY : Springer New York, 1994.

Gennarelli Thomas A and Wodzin Elaine Abbreviated injury scale 2005: update 2008 [Book]. - Barrington : Association for the Advacement of Automotive Medicine, 2008.

Gilat Amos and Subramaniam Vish Numerical methods for engineers and scientits [Book]. - New York : John Wiley & Sons,, 2013. - 3.

Hall Susan J. Basic Biomechanics [Book]. - New York : McGraw-Hill Humanities/Social Sciences/Languages, 2011. - Sixth. - 978-0073376448.

Hayes Wilson C, Erickson Mark S and Power Erik D Forensic Injury Biomechanics [Article] // Annu Rev Biomed Eng.. - 2007.

Hong Youlina Routledfge Handbook of Ergonomics in Sport and Exercise [Book]. - London : Routledge, 2014.

Chow Tai L. Classical Mechanics (second edition) [Book]. - Boca Raton, Florida : CRC Press, 2013.

Chybowski Leszek and Przetakiewicz Wojciech Estimation of the Probability of Head Injury at a Given Abbreviated Injury Scale Level by Means of a Function of Head Injury Criterion [Article] // Syst. Saf. Hum. Tech. Facil. Envirom.. - April 2020. - pp. 91-99.

Mackay M. The increasing importance of the biomechanics of impact trauma. Sadhana [Article]. - 2007. - pp. 397-408.

Mariotti Virzi G [et al.] Head Injury Criterion: Mini Review [Article] // Am J of Biomed Sci & Res.. - Palermo, Italy : Palermo University, October 16, 2019. - p. 5 (5).

McCaw Steve Biomechanics For Dummies [Book]. - Hoboken : John Wiley & Sons Canada, 2014.

Menčík Jaroslav Rázy a vibrace: Základy mechaniky a zmírňování účinků [Book]. - Pardubice : Univerzita Pardubice, 2018.

Nikravesh Parviz E. Planar Multibody Dynamics: Formulation, Programming with MATLAB®, and Applications [Book]. - Boca Raton, Florida : CRC Press, 2018. - Second Edition. - ISBN 9781138096127.

Pascoletti Giulia [et al.] A multibody simulation of a human fall: model creation and validation [Conference] // Procedia Structural Integrity. - 2019. - Vol. Volume 24. - pp. 337-348.

Prasad Priya and Mertz H.S. The position of the United States delegation to the ISO working group 6 on the Use of HIC in the automotive environment, [Article] // SAE 851246. - Washington, D.C. : S.A.E. Government Industry Meeting,, 1985.

Shabana Ahmed A. Dynamics of Multibody Systems [Book]. - University of Illinois, Chicago : Cambridge University Press, 2014. - Fourth. - ISBN 9781107337213.

Shojaati M. Correlation between injury risk and impact severity index ASI [Article] // Swiss Transport Research Conference. - March 20-22, 2003.

Schmitt K.-U. [et al.] Trauma Biomechanics: Accidental injury in traffic and sports [Book]. - Berlin : Springer, 2007.

Simms Ciaran and Wood Denis Pedestrian and Cyclist Impact [Book]. - Dordrecht : Springer, 2009.

Stejskal Vladimír and Brousil Jaromír Mechanika III. [Book]. - Praha : ČVUT, Strojní fakulta, 2001. - ISBN 80-01-02388-5.

Straus Jiří Aplikace forenzní biomechaniky [Book]. - Praha : Police history, 2001.

Strutzenberger Gerda Kinematic and kinetic analyses of human movement with respect to health, injury prevention and rehabilitation aspects [online]. - 02 07, 2011.

Šmiřák Svatopluk Pružnost a plasticita I. [Book]. - Brno : Akademické nakladatelstvá CERM, s.r.o., 2006.

Van Verth James M. Essential Mathematics for Games and Interactive Applications [Book]. - Oakville, Canada : A K Peters Ltd, 2015.

Vesely Vratislav and Vilimek Miloslav Head Injury Biomechanics I - Head and Neck Injury [Article] // BULLETIN OF APPLIED MECHANICS 8 (32). - 2012. - pp. 65-76.

Vetter D. Seminar: Biomechanik und Dummy-Technik [Book]. - Berlin : TU-Berlin, 2000.

Wilde Krzysztof [et al.] On estimation of occupant safety in vehicular crashes into roadside obstacles using non-linear dynamic analysis [Article] // MATEC Web Conf.. - July 12, 2019. - 00022.

Winter David A. Biomechanics and Motor Control of Human Movement [Book]. - Waterloo, Ontario, Canada : John Wiley & Sons, 2009. - 3rd ed..

Zatciorsky V. and Seluyanov V. The mass and inertia characteristics of the main segments of the human body [Journal] // Biomechanics VIII-B: Proceedings of the Eight International Congress of Biomechanics. - 1983. - pp. 1152-1559.

Zatciorsky Vladimir M Kinetics of human motion [Book]. - Champaign, IL : Humen Kinetics, 2002.

LIST OF FIGURES

LIST OF TABLES

weight [kg]	height [cm]	init_angle [°]	ground [-]	point [-]	init_Fx [N]	init_Fy [N]	imp_linV [ms-1]	imp_linA [ms-2]	res_linA [g]	imp_F [N]	HIC [-]	AIS1 [%]	AIS2 [%]	AIS3 [%]	AIS4 [%]	AIS5 [%]	AIS6 [%]
58	165	0	0.6	head	500	0	3.6	720	72.0	3 345	220	26	7	1	0	0	0
58	165	0	0.6	head	1 000	0	4.2	831	83.1	3 862	315	46	15	3	1	0	0
58	165	0	0.6	head	1 500	0	5.0	1 003	100.3	4 659	503	78	37	11	4	0	0
58	165	0	0.6	head	2 000	0	4.4	873	87.3	4 056	356	54	19	4	1	0	0
58	165	0	0.6	head	2 500	0	4.3	853	85.3	3 964	336	50	17	4	1	0	0
58	165	0	0.6	head	3 000	0	4.3	857	85.7	3 981	340	51	17	4	1	0	0
58	165	0	0.6	head	3 500	0	3.3	659	65.9	3 063	176	18	4	0	0	0	0
75	185	0	0.6	head	500	0	3.9	790	79.0	4 126	277	38	11	2	0	0	0
75	185	0	0.6	head	1 000	0	4.5	899	89.9	4 695	383	59	22	5	2	0	0
75	185	0	0.6	head	1 500	0	5.3	1 051	105.1	5 489	566	85	45	15	5	0	0
75	185	0	0.6	head	2 000	0	5.5	1 092	109.2	5 707	624	90	53	19	7	0	0
75	185	0	0.6	head	2 500	0	4.8	956	95.6	4 995	447	70	30	8	3	0	0
75	185	0	0.6	head	3 000	0	4.5	897	89.7	4 684	381	59	22	5	2	0	0
75	185	0	0.6	head	3 500	0	4.5	909	90.9	4 746	393	61	23	6	2	0	0
58	165	0	0.6	head	- 500	0	4.2	831	83.1	3 862	315	46	15	3	1	0	0
58	165	0	0.6	head	- 1 000	0	5.6	1 128	112.8	5 244	676	93	59	23	9	0	0
58	165	0	0.6	head	- 1 500	0	5.6	1 117	111.7	5 191	659	92	57	22	8	0	0
58	165	0	0.6	head	- 2 000	0	5.6	1 124	112.4	5 224	670	93	59	22	8	0	0
58	165	0	0.6	head	- 2 500	0	5.1	1 016	101.6	4 719	520	80	39	12	4	0	0
58	165	0	0.6	head	- 3 000	0	5.6	1 118	111.8	5 197	661	92	58	22	8	0	0
58	165	0	0.6	head	- 3 500	0	5.7	1 131	113.1	5 255	680	93	60	23	9	0	0
75	185	0	0.6	head	- 500	0	4.2	834	83.4	4 358	318	46	15	3	1	0	0
75	185	0	0.6	head	- 1 000	0	6.3	1 262	126.2	6 594	895	99	81	42	18	1	0
75	185	0	0.6	head	- 1 500	0	6.0	1 195	119.5	6 242	780	97	71	32	13	0	0
75	185	0	0.6	head	- 2 000	0	5.9	1 183	118.3	6 178	761	96	69	30	12	0	0
75	185	0	0.6	head	- 2 500	0	4.1	830	83.0	4 335	314	45	15	3	1	0	0
75	185	0	0.6	head	- 3 000	0	5.9	1 184	118.4	6 185	762	96	69	30	12	0	0
75	185	0	0.6	head	- 3 500	0	5.9	1 184	118.4	6 184	762	96	69	30	12	0	0

weight [kg]	height [cm]	init_angle [°]	ground [-]	point [-]	init_Fx [N]	init_Fy [N]	imp_linV [ms-1]	imp_linA [ms-2]	res_linA [g]	imp_F [N]	HIC [-]	AIS1 [%]	AIS2 [%]	AIS3 [%]	AIS4 [%]	AIS5 [%]	AIS6 [%]
58	165	0	0.4	head	500	0	4.3	861	86.1	4 000	344	51	18	4	1	0	0
58	165	0	0.4	head	1 000	0	4.5	900	90.0	4 184	384	59	22	5	2	0	0
58	165	0	0.4	head	1 500	0	4.4	885	88.5	4 115	369	56	20	5	1	0	0
58	165	0	0.4	head	2 000	0	4.2	847	84.7	3 936	330	49	16	3	1	0	0
58	165	0	0.4	head	2 500	0	4.1	822	82.2	3 822	307	44	14	3	1	0	0
58	165	0	0.4	head	3 000	0	4.6	912	91.2	4 237	397	61	24	6	2	0	0
58	165	0	0.4	head	3 500	0	4.1	820	82.0	3 810	304	43	14	3	1	0	0
75	185	0	0.4	head	500	0	4.7	936	93.6	4 892	424	66	27	7	2	0	0
75	185	0	0.4	head	1 000	0	4.8	956	95.6	4 995	450	70	30	8	3	0	0
75	185	0	0.4	head	1 500	0	4.1	815	81.5	4 258	300	42	13	3	1	0	0
75	185	0	0.4	head	2 000	0	4.5	907	90.7	4 737	391	60	23	6	2	0	0
75	185	0	0.4	head	2 500	0	4.6	919	91.9	4 803	405	63	25	6	2	0	0
75	185	0	0.4	head	3 000	0	4.3	865	86.5	4 518	348	52	18	4	1	0	0
75	185	0	0.4	head	3 500	0	4.4	871	87.1	4 550	354	53	19	4	1	0	0
58	165	0	0.4	head	- 500	0	5.0	1 005	100.5	4 672	507	78	38	11	4	0	0
58	165	0	0.4	head	- 1 000	0	5.5	1 101	110.1	5 118	637	91	54	20	7	0	0
58	165	0	0.4	head	- 1 500	0	4.7	937	93.7	4 357	425	66	27	7	2	0	0
58	165	0	0.4	head	- 2 000	0	5.5	1 106	110.6	5 139	643	91	55	20	8	0	0
58	165	0	0.4	head	- 2 500	0	4.7	936	93.6	4 349	424	66	27	7	2	0	0
58	165	0	0.4	head	- 3 000	0	5.6	1 122	112.2	5 213	666	92	58	22	8	0	0
58	165	0	0.4	head	- 3 500	0	5.0	1 004	100.4	4 664	504	78	37	11	4	0	0
75	185	0	0.4	head	- 500	0	6.0	1 196	119.6	6 248	782	97	71	32	13	0	0
75	185	0	0.4	head	- 1 000	0	5.6	1 126	112.6	5 881	672	93	59	23	9	0	0
75	185	0	0.4	head	- 1 500	0	5.1	1 016	101.6	5 305	520	80	39	12	4	0	0
75	185	0	0.4	head	- 2 000	0	5.9	1 189	118.9	6 214	771	97	70	31	12	0	0
75	185	0	0.4	head	- 2 500	0	5.8	1 164	116.4	6 078	730	95	66	27	11	0	0
75	185	0	0.4	head	- 3 000	0	5.0	1 006	100.6	5 257	508	78	38	11	4	0	0
75	185	0	0.4	head	- 3 500	0	5.0	1 004	100.4	5 245	505	78	37	11	4	0	0

weight [kg]	height [cm]	init_angle [°]	ground [-]	point [-]	init_Fx [N]	init_Fy [N]	imp_linV [ms-1]	imp_linA [ms-2]	res_linA [g]	imp_F [N]	HIC [-]	AIS1 [%]	AIS2 [%]	AIS3 [%]	AIS4 [%]	AIS5 [%]	AIS6 [%]
58	165	0	0.2	head	500	0	5.6	1 120	112.0	5 205	664	92	58	22	8	0	0
58	165	0	0.2	head	1 000	0	6.0	1 191	119.1	5 535	774	97	70	31	12	0	0
58	165	0	0.2	head	1 500	0	6.1	1 217	121.7	5 655	817	98	75	35	14	0	0
58	165	0	0.2	head	2 000	0	5.7	1 133	113.3	5 264	683	93	60	23	9	0	0
58	165	0	0.2	head	2 500	0	5.5	1 103	110.3	5 127	639	91	55	20	7	0	0
58	165	0	0.2	head	3 000	0	5.9	1 188	118.8	5 522	770	96	70	31	12	0	0
58	165	0	0.2	head	3 500	0	5.4	1 089	108.9	5 061	619	89	52	19	7	0	0
75	185	0	0.2	head	500	0	6.2	1 231	123.1	6 433	841	98	77	37	15	0	0
75	185	0	0.2	head	1 000	0	8.0	1 606	160.6	8 389	1634	99	99	93	64	29	4
75	185	0	0.2	head	1 500	0	5.7	1 147	114.7	5 992	705	94	63	25	10	0	0
75	185	0	0.2	head	2 000	0	6.3	1 261	126.1	6 589	893	99	81	42	18	1	0
75	185	0	0.2	head	2 500	0	6.2	1 230	123.0	6 427	839	98	77	37	15	0	0
75	185	0	0.2	head	3 000	0	5.8	1 159	115.9	6 056	723	95	65	27	10	0	0
75	185	0	0.2	head	3 500	0	5.8	1 169	116.9	6 107	739	96	67	28	11	0	0
58	165	0	0.2	head	- 500	0	6.0	1 198	119.8	5 570	786	97	72	32	13	0	0
58	165	0	0.2	head	- 1 000	0	7.1	1 411	141.1	6 556	1182	99	95	68	34	5	0
58	165	0	0.2	head	- 1 500	0	7.2	1 436	143.6	6 673	1235	99	97	72	38	6	0
58	165	0	0.2	head	- 2 000	0	7.2	1 440	144.0	6 694	1245	99	97	73	39	7	0
58	165	0	0.2	head	- 2 500	0	6.3	1 266	126.6	5 881	901	99	82	43	18	1	0
58	165	0	0.2	head	- 3 000	0	7.4	1 473	147.3	6 847	1317	99	98	78	43	9	0
58	165	0	0.2	head	- 3 500	0	6.8	1 367	136.7	6 353	1093	99	93	61	29	3	0
75	185	0	0.2	head	- 500	0	7.6	1 516	151.6	7 921	1415	99	99	84	50	14	1
75	185	0	0.2	head	- 1 000	0	7.7	1 538	153.8	8 034	1467	99	99	87	53	16	1
75	185	0	0.2	head	- 1 500	0	7.4	1 483	148.3	7 750	1340	99	98	80	45	10	0
75	185	0	0.2	head	- 2 000	0	7.6	1 524	152.4	7 962	1434	99	99	85	51	15	1
75	185	0	0.2	head	- 2 500	0	6.8	1 351	135.1	7 057	1061	99	91	58	27	2	0
75	185	0	0.2	head	- 3 000	0	7.5	1 494	149.4	7 804	1364	99	98	81	46	11	0
75	185	0	0.2	head	- 3 500	0	6.8	1 353	135.3	7 067	1064	99	91	58	27	2	0